DEPARTMENT OF MATHEMATICS

RESEARCH COMPENDIUM

2022

SRI CHANDRASEKHARENDRA SARASWATHI VISWA MAHAVIDYALAYA

(Deemed to be University u/s 3 of UGC act 1956)

(Accredited with "A" Grade by NAAC)

ENATHUR, KANCHIPURAM - 631 561.


Cabell's Directories
Journal TOCs
EBSCO
ULAKBİM TR DİZİN
ProQuest
Scopus
ELSEVIER
zbMATH
the first resource for mathematics

RESEARCH COMPENDIUM
2022
Contents

S.No.	Journal Details	Page No.
1.	**K.S.Rao, K.Saravanan K.N.Prakasha, I.N.Cangul** Maximum and minimum Degree Energies of p-Splitting and p-Shadow graphs,TWMS J. App. and Eng. Math. V.12, N.1, 2022, pp. 1-10	1
2.	**K.Srinivasa Rao**, Hosoya Polynomial and Wiener Index of King's Graph Type Nanostructure Mukt Shabd Journal, Volume XI, Issue I, Jan 2022 pp 272-282	11
3.	**K.Srinivasa Rao**,N Meenakshi Degree-Based Topological Indices Oftrainagulane,Naveen Anveshan,2022 pp 112-119	22
4.	**P Balaji** Analysis of Marked Graph of Two Machine System Processing Two Part Types Using Sign Incidence Matrix, International Journal of Physical Education, Yoga and Health Sciences, Vol.10, Issue -1 February 2022 pp 307-312	31
5.	**S. SARALA E. GEETHA M. NIRMALA** Numerical Investigation of Heat Transfer & Hall Effects on mhd Nanofluid Flow Past over an Oscillating Plate With Radiation, Journal of Thermal Engineering, Vol. 8, No. 6, pp. 1–15, November 2022	37
6.	**V K Radhakrishnan** Openwares in Teaching Mathematics at Tertiary Level , International Journal of Physical Education, Yoga and Health Sciences, Vol.10, Issue -1 February 2022 pp 313-316	51
7.	**T N Kavitha**, A Comparison With Green's Relation and Our More Special Relations, Research and Reflections on Education, Vol. 20 No. 3A October 2022,pp94-98	56

TWMS J. App. and Eng. Math. V.12, N.1, 2022, pp. 1-10

MAXIMUM AND MINIMUM DEGREE ENERGIES OF p-SPLITTING AND p-SHADOW GRAPHS

K. S. RAO[1], K. SARAVANAN[1], K. N. PRAKASHA[2], I. N. CANGUL[3], §

Abstract. Let v_i and v_j be two vertices of a graph G. The maximum degree matrix of G is given in [2] by

$$d_{ij} = \begin{cases} \max\{d_i, d_j\} & if\ v_i\ and\ v_j\ are\ adjacent \\ 0 & otherwise. \end{cases}$$

Similarly the (i,j)-th entry of the minimum degree matrix is defined by taking the minimum degree instead of the maximum degree above, [1]. In this paper, we have elucidated a relation between maximum degree energy of $p-$shadow graphs with the maximum degree energy of its underlying graph. Similarly, a relation has been derived for minimum degree energy also. We disprove the results $E_M(S'(G)) = 2E_M(G)$ and $E_m(S'(G)) = 2E_m(G)$ given by Zheng-Qing Chu et al. [3] by giving some counterexamples.

Keywords and Phrases: maximum degree energy, minimum degree energy, splitting graph, shadow graph.

Mathematics Subject Classification: 05C50, 05C35

1. Introduction

The adjacency matrix of a graph G is known to be a $\{0,1\}$ matrix with the (i,j)-th entry 1 if v_i and v_j are adjacent, and 0 if v_i and v_j are non-adjacent. Gutman introduced the notion of energy of a graph contingent on adjacency matrix which was emanated by the motivation of Hückel molecular orbital approximation, [5]. He defined the energy of a graph as the sum of the absolute values of eigenvalues of the adjacency matrix. Due to the intensive use of the adjacency matrix, many other graph matrices have been introduced which are related to different properties of graph, see e.g. [4, 7, 9]. Distance matrix,

[1] Department of Mathematics, Sri Chandrasekharendra Saraswathi Viswa Mahavidyalaya, Kanchipuram, Tamilnadu, India.
e-mail: raokonda@yahoo.com; ORCID: https://orcid.org/0000-0002-2357-0933.
e-mail: kadirvelsaravanan@gmail.com; ORCID: https://orcid.org/0000-0001-9373-1993
[2] Department of Mathematics, Vidyavardhaka College of Engineering, Mysuru, India.
e-mail: prakashamaths@gmail.com; ORCID: https://orcid.org/0000-0002-6908-4076.
[3] Department of Mathematics, Faculty of Arts and Science, Bursa Uludag University, 16059, Bursa, Turkey.
e-mail: cangul@uludag.edu.tr; ORCID: https://orcid.org/0000-0002-0700-5774; corresponding author.
§ Manuscript received: March 19, 2021; accepted: August 2, 2021.
TWMS Journal of Applied and Engineering Mathematics, Vol.12, No.1

Randic matrix, Laplacian matrix, partition matrix, sum connectivity matrix, minimum covering matrix etc. are some of such matrices.

Let G be a simple graph with n vertices $\{v_1,\ v_2,\ \cdots,\ v_n\}$ and let d_i be the degree of v_i for $i\ =\ 1,\ 2,\ 3,\ \cdots,\ n$. The maximum degree matrix is defined by Adiga and Smitha in [2] as

$$d_{ij}\ =\ \begin{cases} \max\{d_i, d_j\} & if\ v_i\ and\ v_j\ are\ adjacent \\ 0 & otherwise \end{cases}$$

Let $\mu_1,\ \mu_2,\ \cdots,\ \mu_n$ be the maximum degree eigenvalues of $M(G)$. As the maximum degree matrix is a real symmetric matrix with zero trace, these maximum degree eigenvalues are real with sum equal to zero. The maximum degree energy of a graph G is defined similarly to the classical adjacency energy as

$$E_M(G) = \sum_{i=1}^{n} |\mu_i|\,.$$

It is shown that if the maximum degree energy of a graph is rational, then it must be an even integer [2]. K.Srinivasa Rao, et al. [8] obtained bounds on the maximum degree eigenvalues for a general graph and as well as some frequently used graph classes. Several unicyclic graph classes are defined and their maximum degree eigenvalues and energy are calculated [8].

The minimum degree matrix, [1], is defined similarly to the maximum degree matrix with the change in (i, j)-th entry. Here the (i, j)-th entry is the minimum of the degrees of two adjacent vertices v_i and v_j. Let $\rho_1,\ \rho_2,\ \cdots,\ \rho_n$ be the minimum degree eigenvalues of the minimum degree matrix. The minimum degree energy is defined as

$$E_m(G) = \sum_{i=1}^{n} |\rho_i|\,.$$

Proposition 1.1. [6] *Let $A \in M^m$, $B \in M^n$. Let λ be an eigenvalue of A corresponding to an eigenvector x and μ be an eigenvalue of B corresponding to an eigenvector y. Then $\lambda\mu$ is an eigenvalue of $A \otimes B$ corresponding to the eigenvector $x \otimes y$.*

2. Maximum and minimum degree energy of splitting graphs

A derived graph is a graph which is obtained from a given graph according to some set of rules. One of the derived graphs is called splitting graph. The splitting graph $S^{'}(G)$ of a graph G is obtained by adding a new vertex $u^{'}$ to each vertex u such that $u^{'}$ is adjacent to every vertex that is adjacent to u in G. See Fig. 1 as an example:

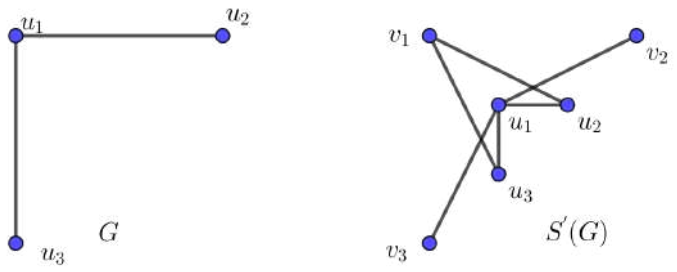

Figure 1

2.1. **Errors.** Zheng-Qing Chu et al., [3], gave the following relations between $E_M(S'(G))$ and $E_M(G)$ and also between $E_m(S'(G))$ and $E_m(G)$. These two results are proven in this paper to be incorrect. We provide some counter-examples which disprove these results. First we recall the erroneous results:

Theorem 2.1. [3] *For a graph G,*

$$E_M(S'(G)) = 2E_M(G).$$

Theorem 2.2. [3] *For a graph G,*

$$E_m(S'(G)) = 2E_m(G).$$

Maximum and minimum degree matrices of G and $S^{'}(G)$ given in Fig. 1 are

$$M(G) = \begin{bmatrix} 0 & 2 & 2 \\ 2 & 0 & 0 \\ 2 & 0 & 0 \end{bmatrix}$$

and

$$m(G) = \begin{bmatrix} 0 & 1 & 1 \\ 1 & 0 & 0 \\ 1 & 0 & 0 \end{bmatrix}$$

and also

$$M(S^{'}(G)) = \begin{bmatrix} 0 & 4 & 4 & 0 & 4 & 4 \\ 4 & 0 & 0 & 2 & 0 & 0 \\ 4 & 0 & 0 & 2 & 0 & 0 \\ 0 & 2 & 2 & 0 & 0 & 0 \\ 4 & 0 & 0 & 0 & 0 & 0 \\ 4 & 0 & 0 & 0 & 0 & 0 \end{bmatrix} \quad \text{and} \quad m(S^{'}(G)) = \begin{bmatrix} 0 & 2 & 2 & 0 & 1 & 1 \\ 2 & 0 & 0 & 2 & 0 & 0 \\ 2 & 0 & 0 & 2 & 0 & 0 \\ 0 & 2 & 2 & 0 & 0 & 0 \\ 1 & 0 & 0 & 0 & 0 & 0 \\ 1 & 0 & 0 & 0 & 0 & 0 \end{bmatrix}.$$

Here $E_M(G) = 5.6569$, $E_m(G) = 2.8284$, $E_M(S'(G)) = 20.3961$ and $E_m(S'(G)) = 10.198$. We can easily observe that $E_M(S'(G)) \neq 2E_M(G)$ and $E_m(S'(G)) \neq 2E_m(G)$. With this example, we can conclude that Theorem 1 and Theorem 2 of [3] are not correct. This is due to the wrong construction of $M(S'(G))$ and $m(S'(G))$ in the proof of Theorem 1 and Theorem 2.

2.2. **Maximum degree energy of p-splitting graphs.** The p-splitting graph $S_p^{'}(G)$ of a graph G is obtained by adding p new vertices, say $\{u_1, u_2, \cdots, u_p\}$, to each vertex u of G such that for $1 \leq i \leq p$, u_i is adjacent to each vertex that is adjacent to u in G.

In this section, we consider an r-regular graph G and obtain the maximum degree energy of a p-splitting graph $S_p^{'}(G)$ in terms of the maximum degree energy of the graph G. Also we obtain the maximum degree energy of p-splitting graphs of some classes of r-regular graphs.

Theorem 2.3. *If G is an r-regular graph, then*

$$E_M({S_p}'(G)) = (p+1)(\sqrt{1+4p})E_M(G).$$

Proof. Let $\{u_1, u_2, \cdots, u_n\}$ be the vertices of an r-regular graph G. Then the maximum degree matrix $M(G)$ is of order n where (i,j)-th entry is given by

$$M(G)(i,j) = \begin{cases} max(d_i, d_j) & \text{if } u_i \text{ and } u_j \text{ are adjacent,} \\ 0 & \text{otherwise.} \end{cases}$$

Let $\{u_i^1, u_i^2, \cdots, u_i^p\}$ be the vertices corresponding to each v_i which are added to G to obtain $S_p^{'}(G)$ such that $N(u_i^1) = N(u_i^2) = \cdots = N(v_i^p) = N(v_i)$ for $i = 1, 2, \cdots, n$. The maximum degree matrix of $S_p^{'}(G)$ is a block matrix of the form

$$M(S_p^{'}(G)) = \begin{bmatrix} (p+1)M(G) & (p+1)M(G) & \cdots & (p+1)M(G) \\ (p+1)M(G) & 0 & \cdots & 0 \\ (p+1)M(G) & 0 & \cdots & 0 \\ \vdots & \vdots & \ddots & \vdots \\ (p+1)M(G) & 0 & \cdots & 0 \end{bmatrix}$$

$$= \begin{bmatrix} p+1 & p+1 & \cdots & p+1 \\ p+1 & 0 & \cdots & 0 \\ p+1 & 0 & \cdots & 0 \\ \vdots & \vdots & \ddots & \vdots \\ p+1 & 0 & \cdots & 0 \end{bmatrix} \otimes M(G) = A \otimes M(G)$$

where O is a null matrix and A= $\begin{bmatrix} p+1 & p+1 & \cdots & p+1 \\ p+1 & 0 & \cdots & 0 \\ p+1 & 0 & \cdots & 0 \\ \cdot & \cdot & \cdots & \cdot \\ p+1 & 0 & \cdots & 0 \end{bmatrix}$.

The spectrum of A is $\begin{pmatrix} 0 & \frac{(p+1)(1+\sqrt{1+4p})}{2} & \frac{(p+1)(1-\sqrt{1+4p})}{2} \\ p-1 & 1 & 1 \end{pmatrix}$.

Hence the spectrum of $M(S_p^{'}(G))$ is

$$\begin{pmatrix} 0\mu_1 & \cdots & 0\mu_n & X\mu_1 & \cdots & X\mu_n & Y\mu_1 & \cdots & Y\mu_n \\ p-1 & \cdots & p-1 & 1 & \cdots & 1 & 1 & \cdots & 1 \end{pmatrix}$$

where $X = \frac{(p+1)(1+\sqrt{1+4p})}{2}$ and $Y = \frac{(p+1)(1-\sqrt{1+4p})}{2}$. Hence

$$\begin{aligned} E_M(S_p^{'}(G)) &= \sum_{i=1}^{n} \left| (p+1)\left(\frac{1 \pm \sqrt{1+4p}}{2}\right)\mu_i \right| \\ &= (p+1)\sum_{i=1}^{n} |\mu_i| \left(\frac{1+\sqrt{1+4p}}{2} + \frac{\sqrt{1+4p}-1}{2}\right) \\ &= (p+1)(\sqrt{1+4p})E_M(G). \end{aligned}$$

□

Corollary 2.1. *If G is a cycle graph of order $n \geq 3$, then*

$$E_M(S_p^{'}(C_n)) = 4(p+1)\sqrt{1+4p}\sum_{k=0}^{n-1}\left|\cos\frac{2k\pi}{n}\right|.$$

Proof. If G is a cycle graph C_n $(n \geq 3)$, then $E_M(C_n) = 4\sum_{k=0}^{n-1}\left|\cos\frac{2k\pi}{n}\right|$, [8]. Since C_n is a 2-regular graph, we have the required result using Theorem 2.3. □

Corollary 2.2. *If G is complete graph of order n, then*

$$E_M(S_p^{'}(K_n)) = 2(p+1)\sqrt{1+4p}(n-1)^2.$$

Proof. If G is the complete graph K_n, then $E_M(K_n) = 2(n-1)^2$, [2]. Since K_n is an $n-1$ regular graph, using Theorem 2.3, we have the required result. □

Corollary 2.3. *If $K_{n,n}$ is a complete bipartite graph, then*

$$E_M(S_p^{'}(K_{n,n})) = 2n^2(p+1)\sqrt{1+4p}.$$

Proof. If G is a complete bipartitie graph, then $E_M(K_{m,n}) = 2\sqrt{mn^3}$ for $m \geq n$, [8]. Therefore $E_M(K_{n,n}) = 2n^2$. Hence by Theorem 2.3, we have the required result. □

Corollary 2.4. *If G is a crown graph on $2n$ vertices, then*

$$E_M(S_p^{'}(G)) = 4(p+1)\sqrt{1+4p}(n-1)^2.$$

Proof. If G is a crown graph on $2n$ vertices then $E_M(G) = 4(n-1)^2$, [8]. Hence by Theorem 2.3, we have the required result. □

2.3. **Minimum Degree Energy of p-Splitting Graphs.** If G is an r-regular graph, then $m(G) = M(G)$. Hence we have the following result:

Theorem 2.4. *If G is an r-regular graph, then*

$$E_m(G) = E_M(G).$$

Theorem 2.5. *If G is an r-regular graph, then*

$$E_m(S_p{}'(G)) = \sqrt{(p+1)^2+4p}E_m(G).$$

Proof. Let $\{u_1,\ u_2,\ \cdots,\ u_n\}$ be the vertices of an r-regular graph G and $m(G)$ be the minimum degree matrix. Let $\{u_i^1,\ u_i^2,\ \cdots,\ u_i^p\}$ be the vertices corresponding to each v_i which are added in G to obtain $S_p^{'}(G)$ such that $N(u_i^1) = N(u_i^2) = \cdots = N(v_i^p) = N(v_i)$, $i = 1,\ 2,\ \cdots,\ n$. Then the minimum degree matrix of $S_p^{'}(G)$ is a block matrix of the form

$$\begin{aligned} m(S_p^{'}(G)) &= \begin{bmatrix} (p+1)m(G) & m(G) & \cdots & m(G) \\ m(G) & O & \cdots & O \\ m(G) & O & \cdots & O \\ \vdots & \vdots & \ddots & \vdots \\ m(G) & O & \cdots & O \end{bmatrix} \\ &= \begin{bmatrix} p+1 & 1 & \cdots & 1 \\ 1 & 0 & \cdots & 0 \\ 1 & 0 & \cdots & 0 \\ \vdots & \vdots & \ddots & \vdots \\ 1 & 0 & \cdots & 0 \end{bmatrix}_{p+1} \otimes m(G) \\ &= A \otimes m(G) \end{aligned}$$

where O is a null matrix and A$=\begin{bmatrix} p+1 & 1 & \cdots & 1 \\ 1 & 0 & \cdots & 0 \\ 1 & 0 & \cdots & 0 \\ \cdot & \cdot & \cdots & \cdot \\ 1 & 0 & \cdots & 0 \end{bmatrix}$. Hence the spectrum of A is

$$\begin{pmatrix} 0 & \frac{p+1+\sqrt{(p+1)^2+4p}}{2} & \frac{p+1-\sqrt{(p+1)^2+4p}}{2} \\ p-1 & 1 & 1 \end{pmatrix}.$$

Now the spectrum of $m(S_p^{'}(G))$ is

$$\begin{pmatrix} 0\mu_1 & \cdots & 0\mu_n & P\mu_1 & \cdots & P\mu_n & Q\mu_1 & \cdots & Q\mu_n \\ p-1 & \cdots & p-1 & 1 & \cdots & 1 & 1 & \cdots & 1 \end{pmatrix}$$

where $P=\dfrac{p+1+\sqrt{(p+1)^2+4p}}{2}$ and $Q=\dfrac{p+1-\sqrt{(p+1)^2+4p}}{2}$. Hence

$$\begin{aligned} E_m(S_p^{'}(G)) &= \sum_{i=1}^{n}\left|\frac{p+1\pm\sqrt{(p+1)^2+4p}}{2}\mu_i\right| \\ &= \sum_{i=1}^{n}|\mu_i|\left(\frac{p+1+\sqrt{(p+1)^2+4p}}{2}+\frac{\sqrt{(p+1)^2+4p}-(p+1)}{2}\right) \\ &= \sqrt{(p+1)^2+4p}E_m(G). \end{aligned}$$

□

Corollary 2.5. *If C_n is the cycle graph of order n ($n \geq 3$), then*

$$E_m(S_p^{'}(C_n)) = 4\sqrt{(p+1)^2+4p}\sum_{k=0}^{n-1}\left|\cos\frac{2k\pi}{n}\right|.$$

Corollary 2.6. *If K_n is the complete graph of order n, then*

$$E_m(S_p^{'}(K_n)) = 2(n-1)^2\sqrt{(p+1)^2+4p}.$$

Corollary 2.7. *If $K_{n,n}$ is complete bipartite graph, then*

$$E_p(S^{'}(K_{n,n})) = 2n^2\sqrt{(p+1)^2+4p}.$$

Corollary 2.8. *If G is crown graph with $2n$ vertices then*

$$E_p(S^{'}(G)) = 4(n-1)^2\sqrt{(p+1)^2+4p}.$$

3. Maximum and minimum degree energies of p-shadow graphs

The shadow graph $D_2(G)$ of a connected graph G is constructed by taking two copies of G say $G^{'}$ and $G^{''}$ and joining each vertex $u^{'}$ in $G^{'}$ to the neighbors of the corresponding $u^{''}$ in $G^{''}$. For example The p-shadow graph $D_p(G)$ of a connected graph G is similarly constructed by taking p copies of G, say $G_1,\ G_2,\ \cdots,\ G_p$ and then joining each vertex u of G_i to the neighbors of the corresponding vertex v in G_j, for $1 \leq i, j \leq p$. For example

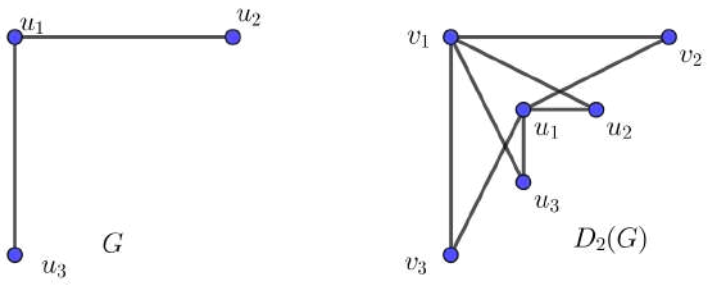

FIGURE 2. The shadow graph of P_3

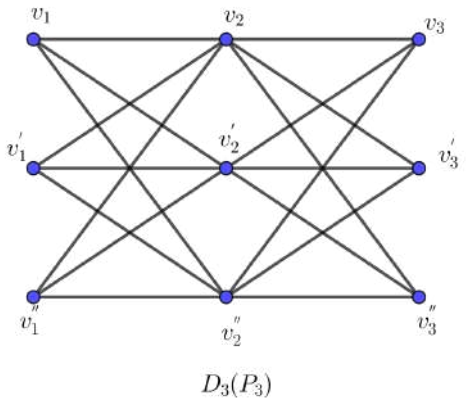

3.1. **Maximum degree energy of p-shadow graphs.**

Theorem 3.1. *For a graph G, we have*

$$E_M(D_p(G)) = p^2 E_M(G).$$

Proof. Let $\{u_1,\ u_2,\ \cdots,\ u_n\}$ be the set of vertices of a graph G. Then the maximum degree matrix of G is the same with the one in the proof of Theorem 2.3. Consider p-copies of graph G, say $G_1,\ G_2,\ \cdots,\ G_p$ with vertices $u_1^1,\ u_2^2,\ \cdots,\ u_n^p$. To obtain $D_p(G)$, each vertex v in G_j is joined to the neighbors of the corresponding vertex v in G_j, for $1 \leq i, j \leq p$. Then $M(D_p(G))$ is a block matrix of order np and it is of the form

$$\begin{aligned} M(D_p(G)) &= \begin{bmatrix} pM(G) & pM(G) & \cdots & pM(G) \\ pM(G) & pM(G) & \cdots & pM(G) \\ pM(G) & pM(G) & \cdots & pM(G) \\ \vdots & \vdots & \ddots & \vdots \\ pM(G) & pM(G) & \cdots & pM(G) \end{bmatrix} \\ &= \begin{bmatrix} p & p & \cdots & p \\ p & p & \cdots & p \\ p & p & \cdots & p \\ \vdots & \vdots & \ddots & \vdots \\ p & p & \cdots & p \end{bmatrix} \otimes M(G) \\ &= pJ_p \otimes M(G). \end{aligned}$$

Since the spectrum of pJ_p is $\begin{pmatrix} 0 & p^2 \\ p-1 & 1 \end{pmatrix}$, the spectrum of $M(D_p(G))$ is

$$\begin{pmatrix} 0\mu_1 & \cdots & 0\mu_n & p^2\mu_1 & \cdots & p^2\mu_n \\ 0 & \cdots & 0 & 1 & \cdots & 1 \end{pmatrix}.$$

Hence we deduce

$$\begin{aligned} E_M(D_p(G)) &= \sum_{i=1}^{n} |p^2\mu_i| \\ &= p^2 E_M(G). \end{aligned}$$

□

In the following corollaries, we obtain the maximum degree energies of shadow graphs of some classes of graphs:

Corollary 3.1. *If G is a cycle graph of order $n \geq 3$, then*

$$E_M(D_p(C_n)) = 4p^2 \sum_{k=0}^{n-1} \left| \cos\left(\frac{2k\pi}{n}\right) \right|.$$

Corollary 3.2. *If G is a complete graph of order n, then*

$$E_M(D_p(K_n)) = 2p^2(n-1)^2.$$

Corollary 3.3. *If $K_{m,n}$ is the complete bipartite graph with $m \geq n$, then*

$$E_M(D_p(K_{m,n})) = 2p^2\sqrt{mn^3}.$$

Proof. Since $E_M(K_{m,n}) = 2\sqrt{mn^3}$ for $m \geq n$ [8], $E_M(D_p(K_{m,n})) = 2p^2\sqrt{mn^3}$. □

Corollary 3.4. *If G is a path graph on n vertices, then*

$$E_M(D_p(P_n)) = 4p^2 \sum_{k=1}^{n} \left| \cos\frac{k\pi}{n+1} \right|.$$

Proof. If G is a path graph on n vertices, then $E_M(P_n) = 4\sum_{k=1}^{n} \left|\cos\frac{k\pi}{n+1}\right|$, [8]. Therefore $E_M(D_p(P_n)) = 4p^2 \sum_{k=1}^{n} \left|\cos\frac{k\pi}{n+1}\right|$. □

Corollary 3.5. *If G is a crown graph with $2n$ vertices, then*

$$E_M(D_p(G)) = 4p^2(n-1)^2.$$

3.2. **Minimum degree energy of p-shadow graphs.** In this section, we obtain the minimum degee energy of a p-shadow graph in terms of minimum degree energy. Also obtained the minimum degree energy of p-shadow graphs of some classes of regular graphs.

Theorem 3.2. *For a graph G, $E_m(D_p(G)) = p^2 E_m(G)$.*

Proof. Let $m(G)$ be the minimum degree matrix of G. Then, mimimum degree matrix of p-shadow graph of G is block matrix of order pn and it is of the form

$$m(D_p(G)) = \begin{bmatrix} p\cdot m(G) & p\cdot m(G) & \cdots & \cdot m(G) \\ p\cdot m(G) & p\cdot m(G) & \cdots & p\cdot m(G) \\ \vdots & \vdots & \ddots & \vdots \\ p\cdot m(G) & p\cdot m(G) & \cdots & p\cdot m(G) \end{bmatrix} = J_p \otimes m(G).$$

Since the spectrum of pJ_p is

$$\begin{pmatrix} 0 & p^2 \\ p-1 & 1 \end{pmatrix},$$

the spectrum of $m(D_p(G))$ is

$$\begin{pmatrix} 0\rho_1 & \cdots & 0\rho_n & m^2\rho_1 & \cdots & m^2\rho_n \\ 0 & \cdots & 0 & 1 & \cdots & 1 \end{pmatrix}.$$

Hence

$$E_m(D_p(G)) = \sum_{i=1}^{n} |p^2\rho_i| = p^2 E_m(G).$$

□

We now obtain the minimum degree energy of shadow graph of some classes of graphs in the following corollaries:

Corollary 3.6. *If G is a cycle graph of order $n \geq 3$, then*

$$E_m(D_p(C_n)) = 4p^2 \sum_{k=0}^{n-1} \left| \cos \frac{2k\pi}{n} \right|.$$

Corollary 3.7. *If G is a complete graph of order n, then*

$$E_m(D_p(K_n)) = 2p^2(n-1)^2.$$

Corollary 3.8. *If G is crown graph with $2n$ vertices, then*

$$E_m(D_p(G)) = 4p^2(n-1)^2.$$

Corollary 3.9. *If $K_{r,s}$ is the complete bipartite graph with $r \geq s$, then*

$$E_m(D_p(K_{r,s})) = 2p^2\sqrt{rs^3}.$$

References

[1] C. Adiga, C. S. Shivakumar Swamy, Bounds on the Largest of Minimum Degree Eigenvalues of Graphs, International Mathematical Forum, 5, (37), (2010), 1823-1831.

[2] C. Adiga, M. Smitha, On Maximum Degree Energy of a Graph, Int. J. Contemp. Math. Sciences, 4, (8) (2009), 385-396.

[3] Z.-Q. Chu, S. Nazeer, T. J. Zia, I. Ahmed, S. Shahid, Some New Results on Various Graph Energies of the Splitting Graph, Journal of Chemistry, 2019, Article ID 7214047, 12 pages.

[4] G. K. Gok, Some bounds on the Seidel energy of graphs, TWMS J. App. Eng. Math., 9, (4) (2019), 949-956.

[5] I. Gutman, The energy of a graph, Ber. Math.-Statist. Sekt. Forsch. Graz, (100-105): 103, (22), (1978), 10. Steiermaerkisches Mathematisches Symposium (Stift Rein, Graz), (1978).

[6] R. A. Horn, C. R. Johnson, Topics in Matrix Analysis, Cambridge Univ. Press, Cambridge, (1991).

[7] M. H. Nezhaad, M. Ghorbani, Seidel borderenergetic graphs, TWMS J. App. Eng. Math., 10, (2), (2020), 389-399.

[8] K. S. Rao, K. N. Prakasha, K. Saravanan, I. N. Cangul, Maximum Degree Energy, Advanced Studies in Contemporary Mathematics, 31, (1), (2021), 49-66.

[9] E. Sampathkumar, S. V. Roopa, K. A. Vidya, M. A. Sriraj, Partition energy of some trees and their generalized complements, TWMS J. App. and Eng. Math., 10, (2), (2020), 521-531.

K. Srinivasa Rao completed his Ph.D in mathematics at Aacharya Nagarjuna University, M.Phil. at Madurai Kamaraj University, M.Sc. at JNT university, and PGDCS at the University of Hyderbad. His primary research focuses on Chemical Graph Theory and Algebra. Currently, he is working as a professor of mathematics at Sri Chandrasekharendra Saraswathi Viswa Mahavidyalaya, Kanchipuram, India.

K. Saravanan is a research scholar at Sri Chandrasekharendra Saraswathi Viswa Mahavidyalaya (Deemed to be University), Kanchipuram, India. He obtained his bachelor degree and master degree in mathematics at the University of Madras, India. Presently, he is working in the Department of Mathematics, Sri Chandrasekharendra Saraswathi Viswa Mahavidyalaya (Deemed to be University), Kanchipuram, India.

K. N. Prakasha for the photography and short autobiography, see TWMS J. App. and Eng. Math. V.9, N.4, 2019.

Ismail Naci Cangul for the photography and short autobiography, see TWMS J. App. and Eng. Math., V.6, N.2, 2016.

HOSOYA POLYNOMIAL AND WIENER INDEX OF KING'S GRAPH TYPE NANOSTRUCTURE

K. Srinivasa Rao

Department of Mathematics
Sri Chandrasekharendra Saraswathi Viswa Mahavidyalaya
Kanchipuram, Tamilnadu India.
raokonda@yahoo.com

Abstract

In this paper, we obtained Hosoya polynomial and Wiener index of $(1 \times n)$, $(2 \times n)$, $(3 \times n)$ and $(4 \times n)$ King's graph type nanostructures and extended this to $(n \times n)$ King's graph.

AMS 2010 Subject Classification Number: 05C07, 05C30, 05C38, 05C76
Keywords: Wiener Index, Hosoya Polynomial, King's graph.

1 Introduction

Now a days graph theory has many applications in such different fields as computer science, engineering, biology etc., and particularly in chemistry. In 1947, Harold Wiener published a paper [1], entitled Structural Determination of Paraffin Boiling Points. In this work, Wiener Index or Wiener number was introduced for the first time and he used his index for the calculation of the boiling points of alkanes. Let G be a connected graph, then the Wiener Index of the graph $G(V, E)$ is defined as :

$$W(G) = \sum_{\{u,v\} \subset V(G)} d(u, v)$$

where $d(u, v)$ is the minimum of the lengths of all $u - v$ paths in G, i.e., the shortest path between the vertices u and v. The Hosoya polynomial (also called Wiener polynomial) of G is defined as

$$H(G, x) = \sum_{\{u,v\} \subset V(G)} x^{d(u,v)}.$$

It is clear that

$$H(G, x) = \sum_{k \geq 0} d(G, k) x^k,$$

where $d(G, k)$ is the number of pairs (u, v) of vertices of G such that $d(u, v) = k$. The Hosoya polynomial of a vertex v of G is defined as

$$H(v, G; x) = \sum_{k \geq 1} d(v, G, k) x^k,$$

in which $d(v, G, k)$ is the number of all vertices u belonging to $V(G)$, such that $d(u, v) = k$. The Wiener index of G can be obtained directly from the Hosoya polynomial of G as follows:

$$W(G) = \frac{d}{dx}(H(G, x))|_{x=1}.$$

Gutman. et.al [2] obtained Hosoya polynomial for a number of homologeous series of unbranched catcondensed benenoid systems using recursive method. In [3]-[4], Rao, N.P. and Prasanna, A.L., obtained formulas for Wiener indices of chemical graphs formed of concatenated 5-cycles. Ali.A.Ali and Ahmed M. Ali [5] Hosoya polynomials of several types of graphs consisting of concatenated pentagonal rings are obtained using induction. Recently K.S.Rao, et.al [6], obtained Hosoya polynomials of different types of graphs consisting of concatenated octachain rings are obtained. In this paper,we calculated Hosoya polynomial and Wiener index of $(1 \times n)$, $(2 \times n)$, $(3 \times n)$, $(4 \times n)$, $(5 \times n)$ King's graph type nanostructures and extended this to $(n \times n)$.

1.1 King's Graph

King's graph is a graph that represents all legal moves of the king chess piece on a chessboard where each vertex represents a square on a chessboard and each edge is a legal move. More specifically, an $(m \times n)$ king's graph is a king's graph of an $(m \times n)$ chessboard.It is the map formed from the squares of a chessboard by making a vertex for each square and an edge for each two squares that share an edge or a corner. For $(n \times n)$ King's graph, the total number of vertices is $(n - 1)^2$ and the number of edges $2n(2n + 1)$. We obtained the Hosoya Polynomial and Wiener index for the graph $G(1 \times n, S_1)$, consisting of one row and n columns of King's graph in the next theorem.

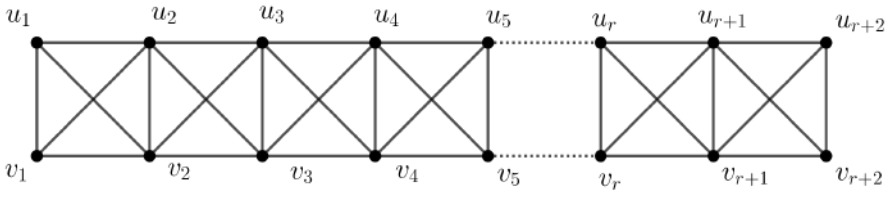

Figure 1: $G(1 \times n, S_1)$

Theorem 1.1. *The Hosoya polynomial of the graph* $G(1 \times n, S_1)$ *is given by*

$$H[G(1 \times n, S_1)] = (5n+1)x + 4\sum_{k=1}^{n-1}(n-k)x^{k+1}, n \geq 2$$

Proof. We prove this theorem using Mathematical induction on n for $n \geq 2$.
For $n = 2$, we have by direct calculation, the Hosoya polynomial is $11x + 4x^2$.Also, $H[G(1 \times 2, S_1)] = 11x + 4\sum_{k=1}^{1}(2-k)x^{k+1} = 11x + 4x^2$. Thus, the theorem is true for $n = 2$.
Let us assume that the theorem is true for $n = r \geq 2$ and we prove this is true for $n = r+1$.
From the figure 1,

$$H[G(1 \times (r+1), S_1)] = H[G(1 \times r, S_1)] + g(x) \tag{1}$$

where $g(x) = \sum_{i=1}^{2}(H[a_i, G(1 \times (r+1), S_1)]) - x + 4x^{r+1}$ and $a_1 = u_{r+2}, a_2 = v_{r+2}$.
But by the symmetry $H[u_{r+2}, G(1 \times (r+1), S_1)] = H[v_{r+2}, G(1 \times (r+1), S_1)]$
Therefore, $g(x) = H[u_{r+2}, G(1 \times (r+1), S_1)] - x + 4x^{r+1}$.
Also, $H[u_{r+2}, G(1 \times (r+1), S_1)] = 3x + 2\sum_{k=1}^{r-1}x^{k+1}$.
Therefore,

$$\begin{aligned} g(x) &= 6x + 4\sum_{k=1}^{r-1}x^{k+1} - x + 4x^{r+1} \\ &= 5x + 4\sum_{k=1}^{r-1}x^{k+1} = 5x + 4\sum_{k=1}^{r}x^{k+1} \end{aligned}$$

Therefore, from (1)

$$\begin{aligned} H[G(1\times(r+1),S_1)] &= H[G(1\times r,S_1)] + g(x) \\ &= (5r+1)x + 4\sum_{k=1}^{r-1}(r-k)x^{k+1} + 5x + 4\sum_{k=1}^{r}x^{k+1} \\ &= [5(r+1)+1)x + 4\sum_{k=1}^{r}[(r+1)-k]x^{k+1} \end{aligned}$$

Hence the result is true for all $n \geq 2$. Thus we have$H[G(1\times n,S_1)], n \geq 2$. The Hosoya polynomial for $G(1\times 1,S_1) = 6x$. Hence we have the Hosoya polynomial for $H[G(1\times n,S_1)]$ for all natural numbers n. □

Theorem 1.2. *The Wiener index of the graph* $G(1\times n,S_1)$ *is given by*

$$W(G(1\times n,S_1)) = \frac{1}{3}\left(2n^3+6n^2+7n+3\right), n \geq 2$$

Proof. Wiener index can be obtained by taking derivative of $H[G(1\times n,S_1)]$ with respect to x and substituting $x = 1$.

$$\begin{aligned} W(G(1\times n,S_1)) &= \frac{d}{dx}\left(H[G(1\times n,S_1)]\right)_{x=1} \\ &= (5n+1) + 4\sum_{k=1}^{n-1}(n-k)(k+1) \\ &= (5n+1) + \frac{2}{3}(n^3+3n^2-4n) \\ &= \frac{1}{3}\left(2n^3+6n^2+7n+3\right), n \geq 2 \end{aligned}$$

By direct calculation $W[G(1\times n,S_1)]$ =6. Thus we obtained $W(G(1\times n,S_1))$ for all natural numbers. □

Here, we consider the structure S_2 consisting of 2 rows and n columns of King's graph, i.e, $G(2\times n,S_1)$ and obtained Hosoya polynomial and Wiener index.

Theorem 1.3. *The Hosoya polynomial of the graph* $G(2\times n,S_2)$ *is given by*

$$H[G(2\times n,S_2)] = (9n+2)x + (12n-8)x^2 + 9\sum_{k=2}^{n-1}(n-k)x^{k+1}, n \geq 3$$

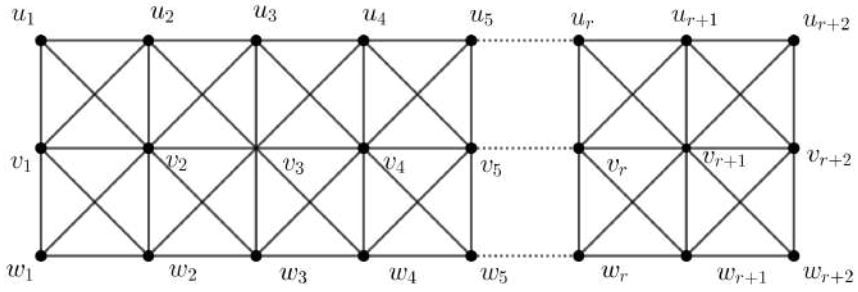

Figure 2: $G(2 \times n, S_2)$

Proof. We prove this theorem using Mathematical induction on n for $n \geq 3$
For $n = 3$, we have by direct calculation, the Hosoya polynomial is $29x+28x^2+9x^3$.Also $H[G(2 \times 3, S_2)] = 29x + 28x^2 + 9x^3$. Hence the theorem is true for $n = 3$.
Let us assume that the theorem is true for $n = r \geq 3$ and we prove this is true for $n = r+1$.
From the figure 2,

$$H[G(2 \times (r + 1), S_2)] = H[G(2 \times r, S_2)] + g(x) \tag{2}$$

where $g(x) = \sum_{i=1}^{3} (H[a_i, G(2 \times (r + 1), S_2)]) - 2x - x^2 + 9x^{r+1}$ and $a_1 = u_{r+2}, a_2 = v_{r+2}, a_3 = w_{r+2}$. But by the symmetry $H[u_{r+2}, G(2 \times (r+1), S_2)] = H[w_{r+2}, G(2 \times (r + 1), S_2)]$
Therefore,
$g(x) = 2H[u_{r+2}, G(2\times(r+1), S_2)]+H[v_{r+2}, G(2\times(r+1), S_2)]-2x-x^2+9x^{r+1}$. Also, $H[u_{r+2}, G(2 \times (r+1), S_2)] = 3x+5x^2+3\sum_{k=2}^{r-1} x^{k+1}$. and $H[v_{r+2}, G(2 \times (r+1), S_2)] = 5x + 3\sum_{k=1}^{r-1} x^{k+1}$.
Therefore,

$$\begin{aligned} g(x) &= 6x + 10x^2 + 6\sum_{k=2}^{r-1} x^{k+1} + 5x + 3\sum_{k=2}^{r-1} x^{k+1} - 2x - x^2 + 9x^{r+1} \\ &= 11x + 13x^2 + 9\sum_{k=2}^{r-1} x^{k+1} - 2x - x^2 + 9x^{r+1} \\ &= 9x + 12x^2 + 9\sum_{k=2}^{r} x^{k+1} \end{aligned}$$

Therefore,

$$\begin{aligned} H[G(2\times(r+1),S_2)] &= H[G(2\times r,S_2)] + g(x) \\ &= (9r+2)x + (12r-8)x^2 + 9\sum_{k=2}^{r-1}(r-k)x^{k+1} + 9x + 12x^2 + 9\sum_{k=2}^{r}x^{k+1} \\ &= [9(r+1)+2]x + [12(r+1)-8]x^2 + 9\sum_{k=2}^{r}[(r+1)-k]x^{k+1} \end{aligned}$$

Hence the result is true for all $n \geq 3$. Thus we obtain $H[G(2\times n, S_2)]$ for all $n \geq 3$. The Hosoya polynomial of $G(2\times 1, S_2) = 11x + 4x^2$ and $G(2\times 2, S_2) = 20x + 16x^2$. Hence we have the Hosoya polynomial of $G(2\times n, S_2)$ for all natural numbers n. □

Theorem 1.4. *The Wiener index of the graph $G(2\times n, S_2)$ is given by*

$$W(G(2\times n, S_2)) = \frac{1}{2}\left(3n^3 + 9n^2 + 18n + 8\right), n \geq 3$$

Proof. The proof of the theorem is similar to the proof of Theorem 1.2

□

By direct calculation $W[G(2\times 1, S_2)]$ =19 and $W[G(2\times 2, S_2)]$ =52 Thus we obtained $W(G(2\times n, S_2))$ for all natural numbers.
Here, we consider the structure S_3 consisting of 3 rows and n columns of King's graph, i.e, $G(3\times n, S_3)$ and obtained Hosoya polynomial and Wiener index.

Theorem 1.5. *The Hosoya polynomial of the graph $G(3\times n, S_3)$ is given by*

$$H[G(3\times n, S_3)] = (13n+3)x + (20n-12)x^2 + (21n-33)x^3 + 16\sum_{k=3}^{n-1}(n-k)x^{k+1}, n \geq 4$$

Proof. We prove this theorem using Mathematical induction on n for $n \geq 4$
For $n = 4$, we have by direct calculation, the Hosoya polynomial is $55x + 68x^2 + 51x^3 + 16x^4$. Also $H[G(3\times 4, S_3)] = 55x + 68x^2 + 51x^3 + 16x^4$. Hence the theorem is true for $n = 4$.
Let us assume that the theorem is true for $n = r \geq 4$ and we prove this is true for $n = r+1$. From the figure 3,

$$H[G(3\times(r+1), S_3)] = H[G(3\times r, S_3)] + g(x) \tag{3}$$

where $g(x) = \sum_{i=1}^{4}(H[a_i, G(3\times(r+1), S_3)]) - 3x - 2x^2 - 9x^3 + 16x^{r+1}$ and $a_1 = u_{r+2}, a_2 = v_{r+2}, a_3 = w_{r+2}, a_4 = x_{r+2}$. But by the symmetry

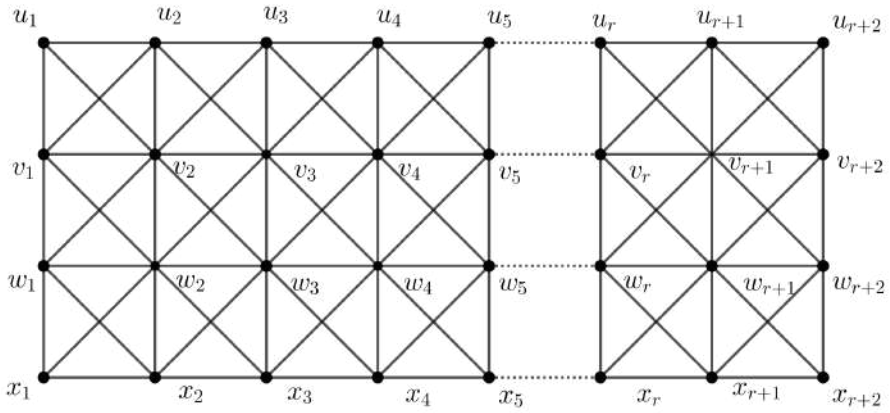

Figure 3: $G(3 \times n, S_3)$

$$H[u_{r+2}, G(3 \times (r+1), S_3)] = H[x_{r+2}, G(3 \times (r+1), S_3)]$$
$$H[v_{r+2}, G(3 \times (r+1), S_3)] = H[w_{r+2}, G(3 \times (r+1), S_3)]$$

Therefore,

$g(x) = 2H[u_{r+2}, G(3\times(r+1), S_3)]+2H[v_{r+2}, G(3\times(r+1), S_3)]-3x-2x^2-x^3+16x^{r+1}$

Also, $H[u_{r+2}, G(3 \times (r+1), S_3)] = 3x + 5x^2 + 7x^3 + 4\sum_{k=3}^{r-1} x^{k+1}$. and
$H[v_{r+2}, G(3 \times (r+1), S_3)] = 5x + 6x^2 + 4\sum_{k=2}^{r-1} x^{k+1}$.
Therefore,

$$\begin{aligned} g(x) &= 16x + 22x^2 + 22x^3 + 16\sum_{k=3}^{r-1} x^{k+1} - 3x - 2x^2 - x^3 + 16x^{r+1} \\ &= 13x + 20x^2 + 21x^3 + 16\sum_{k=3}^{r-1} x^{k+1} + 16x^{r+1} \end{aligned}$$

Therefore,

$$\begin{aligned} H[G(3 \times (r+1), S_3)] &= H[G(3 \times r, S_3)] + g(x) \\ &= (13r+3)x + (20r-12)x^2 + (21r-33)x^3 + 16\textstyle\sum_{k=3}^{r-1}(r-k)x^{k+1} \\ &\quad +13x + 20x^2 + 21x^3 + 16\textstyle\sum_{k=3}^{r-1} x^{k+1} + 16x^{r+1} \\ &= [13(r+1)+3]x + [20(r+1)-12]x^2 + [21(r+1)-33]x^3 \\ &\quad +16\textstyle\sum_{k=3}^{r-1}[(r+1)-k]x^{k+1} \end{aligned}$$

Hence the result is true for all $n \geq 4$. Thus we obtain $H[G(3 \times n, S_3)]$ for all $n \geq 4$. $\square$

The Hosoya polynomial of $G(3 \times 1, S_3) = 16x + 8x^2 + 4^3$, $G(3 \times 2, S_3) = 29x + 28x^2 + 9x^3$ and $G(3 \times 3, S_3) = 42x + 48x^2 + 30x^3$. Hence we have the Hosoya polynomial of $G(3 \times n, S_3)$ for all natural numbers n.

Theorem 1.6. *The Wiener index of the graph $G(3 \times n, S_3)$ is given by*

$$W(G(3 \times n, S_3)) = \frac{1}{3}\left(8n^3 + 24n^2 + 28n + 120\right), n \geq 4$$

By direct calculation, $W(G(3 \times 1, S_3))$=44, $W(G(3 \times 2, S_3))$=112, and $W(G(3 \times 3, S_3))$=228. Thus we obtain, $W(G(3 \times n, S_3))$ for all natural numbers n.
Here we consider the structure S_4 consisting of 4- rows and n-columns of King's graph and obtained the Hosoya polynomial and Wiener index.

Theorem 1.7. *The Hosoya polynomial of the graph $G(4 \times n, S_4)$, $\forall\ n \geq 5$ is given by*

$$H[G(4\times n, S_4)] = (17n+4)x+(28n-16)x^2+(33n-48)x^3+(32n-80)x^4+25\sum_{k=4}^{n-1}(n-k)x^{k+1}$$

Proof. We prove this theorem using Mathematical induction on n for $n \geq 5$
For $n = 5$, we have by direct calculation, the Hosoya polynomial is $89x+124x^2+117x^3+80x^4+25x^5$. Also $H[G(4 \times 5, S_4)] = 89x + 124x^2 + 117x^3 + 80x^4 + 25x^5$. Hence the theorem is true for $n = 5$.
Let us assume that the theorem is true for $n = r \geq 5$ and we prove this is true for $n = r+1$. From the figure 4,

$$H[G(4 \times (r+1), S_4)] = H[G(4 \times r, S_4)] + g(x) \tag{4}$$

where $g(x) = \sum_{i=1}^{5}\left(H[a_i, G(4 \times (r+1), S_4)]\right) - 4x - 3x^2 - 2x^3 - x^4 + 25x^{r+1}$ and $a_1 = u_{r+2}, a_2 = v_{r+2}, a_3 = w_{r+2}, a_4 = x_{r+2}$ and $a_5 = y_{r+2}$ But by the symmetry

$$H[u_{r+2}, G(4 \times (r+1), S_4)] = H[y_{r+2}, G(4 \times (r+1), S_4)]$$
$$H[v_{r+2}, G(4 \times (r+1), S_4)] = H[x_{r+2}, G(4 \times (r+1), S_4)]$$

Therefore,

$$g(x) = 2H[u_{r+2}, G(4\times(r+1), S_4)] + 2H[v_{r+2}, G(4 \times (r+1), S_4)] + H[w_{r+2}, G(4 \times (r+1), S_4)] - 4x - 3x^2 - 2x^3 - x^4 + 25x^{r+1}$$

Also,

$$H[u_{r+2}, G(4 \times (r+1), S_4)] = 3x + 5x^2 + 7x^3 + 9x^4 + 5\sum_{k=4}^{r-1} x^{k+1}$$

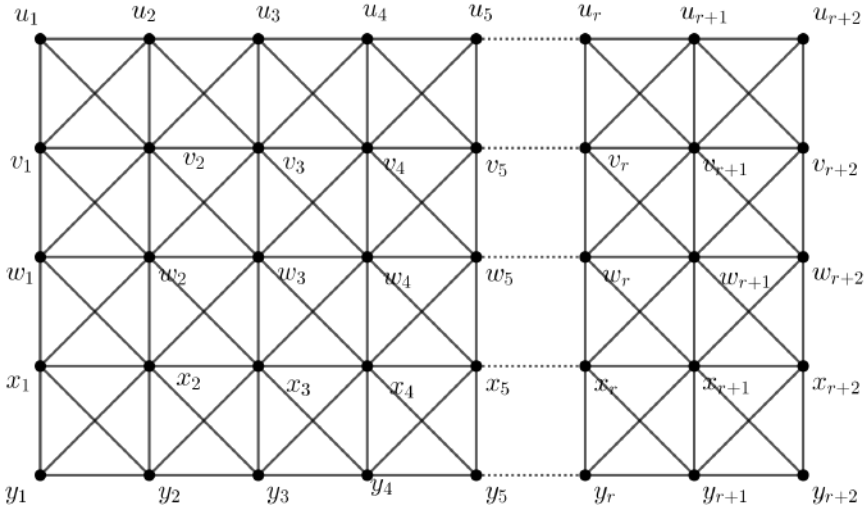

Figure 4: $G(4 \times n, S_4)$

$$H[v_{r+2}, G(4 \times (r+1), S_4)] = 5x + 6x^2 + 8x^3 + 5x^4 + 5\sum_{k=4}^{r-1} x^{k+1}$$

$$H[w_{r+2}, G(4 \times (r+1), S_4)] = 5x + 9x^2 + 5x^3 + 5x^4 + 4\sum_{k=4}^{r-1} x^{k+1}$$

Therefore,

$$\begin{aligned} g(x) &= 6x + 10x^2 + 14x^3 + 18x^4 + 10\textstyle\sum_{k=4}^{r-1} x^{k+1} + 10x + 12x^2 + 16x^3 \\ &\quad +10x^4 + 10\textstyle\sum_{k=4}^{r-1} x^{k+1} + 5x + 9x^2 + 5x^3 + 5x^4 + 5\sum_{k=4}^{r-1} x^{k+1} \\ &\quad -4x - 3x^2 - 2x^3 - x^4 + 25x^{r+1} \\ &= 17x + 28x^2 + 33x^3 + 32x^4 + 25\textstyle\sum_{k=4}^{r-1} x^{k+1} + 25x^{r+1} \end{aligned}$$

Therefore,

$$\begin{aligned} H[G(4 \times (r+1), S_4)] &= H[G(4 \times r, S_4)] + g(x) \\ &= (17r+4)x + (28r-16)x^2 + (33r-48)x^3 \\ &\quad +(32r-80)x^4 + 25\textstyle\sum_{k=4}^{r-1}(r-k)x^{k+1} + 17x + 28x^2 \\ &\quad +33x^3 + 32x^4 + 25\textstyle\sum_{k=4}^{r-1} x^{k+1} + 25x^{r+1} \\ &= [17(r+1)+4]x + [28(r+1)-16]x^2 + [33(r+1)-48]x^3 \\ &\quad +[32(r+1)-80]x^4 + 25\textstyle\sum_{k=4}^{r}[(r+1)-k]x^{k+1} \end{aligned}$$

Hence the result is true for all $n \geq 5$. Thus we obtain $H[G(4 \times n, S_4)]$ for all $n \geq 5$. $\square$

The Hosoya polynomial of $G(4 \times 1, S_4) = 21x + 12x^2 + 8x^3$, $G(4 \times 2, S_4) = 38x + 40x^2 + 18x^3 + 9x^4$,$G(4 \times 3, S_4) = 55x + 68x^2 + 51x^3 + 16x^4$ and $G(4 \times 4, S_4) = 72x + 96x^2 + 84x^3 + 48x^4$ Hence we have the Hosoya polynomial of $G(4 \times n, S_4)$ for all natural numbers n.

Theorem 1.8. *The Wiener index of the graph* $G(4 \times n, S_4)$ *is given by*

$$W(G(4 \times n, S_4)) = \frac{1}{6}\left(25n^3 + 75n^2 + 350n + 48\right), n \geq 5$$

By direct calculation, $W(G(4 \times 1, S_4))$=85, $W(G(4 \times 2, S_4))$=208, and $W(G(4 \times 3, S_4))$=408 and $W(G(4 \times 4, S_4))$=708. Thus we obtain, $W(G(4 \times n, S_4))$ for all natural numbers n.

Finally we consider the graph $G(n \times n, S_n)$ consisting of n- rows and n -columns of King's graph as shown in the fig.5 and the Hosoya polynomial, Wiener index are given in the following theorems.

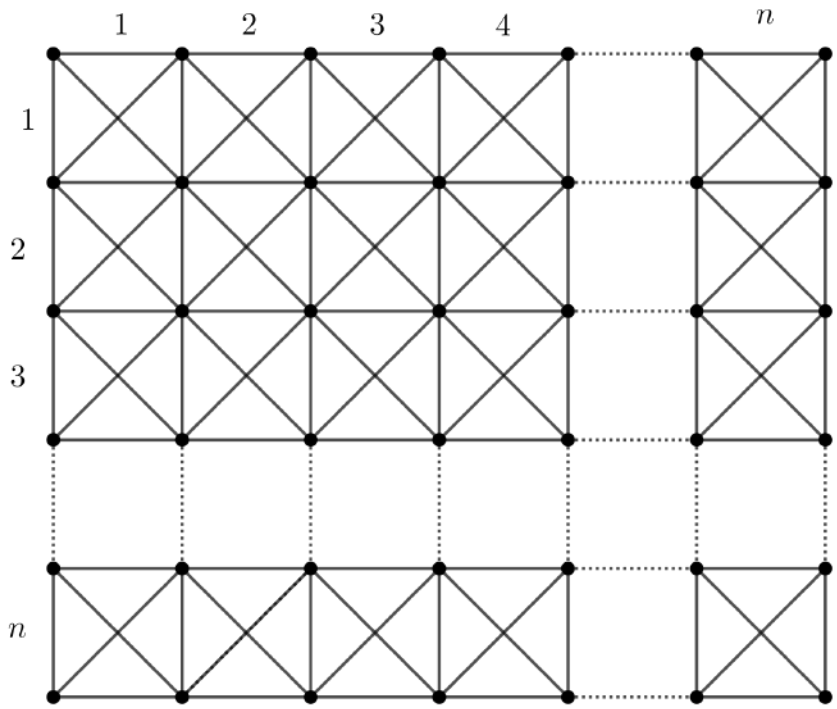

Figure 5: $G(n \times n, S_n)$

Theorem 1.9. *The Hosoya polynomial of the graph $G(n \times n, S_n)$ is given by*

$$H[(n \times n, S_n)] = 2\sum_{k=0}^{n-1}(k+1)(n-k)(2n-k+1)x^{k+1}$$

Theorem 1.10. *The Wiener index of the graph $G(n \times n, S_n)$ is given by*

$$W[(n \times n, S_n)] = \frac{1}{30}(7n^5 + 35n^4 + 65n^3 + 55n^2 + 18n)$$

References

[1] H. Wiener, Structural determination of paraffin boiling points, Journal of American Chemical Society ,(1) 69 , (1947) 17-20..

[2] Ivan Gutman, et.al, On Hosoya polynomial of Benzenoid graphs, Communication in Mathematical and in Computer Chemistry 43(2001), 49-66.

[3] N. Prabhakara Rao, K. Lavanya Lakshmi, A. Laxmi Prasanna, Wiener indices of pentachains, National Conference on Discrete Mathematics and its Applications, Madurai, India, (2007) 384?387.

[4] N. Prabhakara Rao, A. Laxmi Prasanna, On the Wiener index of pentachains, Appl. Math. Sci. 2 (2008) 2443?2457

[5] Ali.A Ali, Ahmed M. Ali, Hosoya polynomial of Pentachains, MATCH Commun. Math. Comput. Chem. 65 (2011) 807-819

[6] K. Srinivasa Rao, B. Amudha, Ismail Naci Cangul, Hosoya Polynomials of concatenated octachains, Advanced Studies in Contemporary Mathematics 30 (2020), No. 4, pp. 609 - 622

DEGREE-BASED TOPOLOGICAL INDICES OFTRIANGULANE

K.Srinivasa Rao[1], N.Meenakshi[2]
[1]Department of Mathematics, Sri ChandrasekharendraSaraswathiViswaMahavidyalaya Enathur, Kanchipuram, Tamilnadu, India
[2]Department of Mathematics, Sri Sankara Arts and ScienceCollege, Enathur, Kanchupuram, Tamilnadu, India

ABSTRACT:-For a molecular graph G=(V,E), a general form of vertex-degree based topological indices is defined as $TI(G) = \sum_{uv \in E(G)} \emptyset(d(u), d(v))$ where $\emptyset$ is non-negative and real two variable function and d(v) denotes the degree of the vertex v. In this paper, we calculated the Harmonic index, Augmented Zagreb Index, Geometric-arithmetic Index,Randic connectivity index, and Zagreb indices of Triangulane.

Keywords: Topological indices, Molecular graph, Triangulane

1. INTRODUCTION

A molecular graph is a simplegraph such that its vertices correspond to the atoms andthe edge to the bonds of a molecule. Let $G= (V, E)$ be a finite, connected, simple graph.We denote the degree of a vertex v in G by d_v. A topological index of G is a real numberrelated to G. It does not depend on the labelling or pictorial representation of a graph.[1] The wiener index W(G) is the first distance-based topological index defined as $W(G) = \sum_{u,v \in (G)} d(u,v) = \frac{1}{2}\sum_{u,v \in V(G)} d(u,v)$ withthe summation runs over all pairs of vertices of G.

[2, 3]A topological index of a chemical compound is an integer, derived following a certain rule, which can be used to characterize the chemical compound and predict certain physiochemical properties like boiling point, molecular weight, density, refractive index, and so forth.

The topological indices and graph invariants are based on the distance between vertices of a graph are widely used for characterizing molecular graphs, establishing relationships betweenthe structure and properties of molecules, predicting biological activity of chemicalcompounds, and making their chemical applications. The Wiener index is one of themost used topological indices with a high correlation with many physical and chemical indices of molecular compounds. [4]Recentlya new vertex – degree –based molecular structure descriptor was put forward, the Somborindex is defined as

$$SO(G) = \sum_{u,v \in E(G)} \sqrt{d_u^2 + d_v^2}.$$

[5]Cruz,GutmanandRadacharacterizedthegraphsextremalwithrespecttothisindex over

the chemical graphs,chemical trees and hexagon systems (see [6]). In [7],the chemical importance of the Sombor index has been investigated and it is shown that thisindex is useful in predicting Physico-chemical properties with high accuracy compared tosome well-established and often used indices. Also, a sharp upper bound for the Somborindex among all molecular trees with fixed numbers of vertices hasbeen obtained, and thosemolecular trees achieving the extremal value has characterized.[8]In some novel, lower and upper bounds of the Sombor index of graphs haspresented by using some graph parameters, especially, maximum and minimum degree.Moreover, several relations on theSombor index with the first and second Zagreb indices ofgraphs were obtained. [9]The mathematical relations between the Sombor index and some otherwell-knowndegree-baseddescriptorswere investigated.

2. Topological indices:

In this paper, we calculated Harmonic Index, Augmented Zagreb Index, Geometric-arithmetic Index, Randic connectivity index, and Zagreb indices of Triangulane.

2.1. Harmonic Index

In the 1980s, SiemionFajtlowicz created a computer program for theautomatic generation of conjectures in graph theory. [10]Then he examined the possible relations between countless graph invariants, among which there was a vertex-degree-based quantity

$$H(G) = \sum_{u,v \in E(G)} \frac{2}{d_u(G) + d_v(G)}$$

With a single exception [11] H(G) did not attract anybody's attention, especially not of chemists. [12,13]Only in 2012, Zhang re-introduced this quantity, and called it the Harmonic index. His works were followed by the recent paper.[14] No chemical applications of the harmonic index were reported so far, but, knowing the present situation in mathematical chemistry, such researchers are very much to be expected.

2.2. AugmentedZagreb Index

Motivated by the success of the ABC index,[15] Furtula et al. put forward its modified version, which they somewhat inadequately named the Augmented Zagreb index. It is defined as

$$AZI(G) = \sum_{u,v \in E(G)} \left(\frac{d_u(G).d_v(G)}{d_u(G) + d_v(G) - 2} \right)^3$$

2.3. Geometric-Arithmetic Index

Another recently conceived vertex-degree-based topological index utilizes the difference between the geometric and arithmetic means is defined as

$$GA(G) = \sum_{u,v \in E(G)} \frac{\sqrt{d_u(G).d_v(G)}}{\frac{1}{2}[d_u(G) + d_v(G)]}$$

Where, $\sqrt{d_u(G).d_v(G)}$ and $\frac{1}{2}[d_u(G) + d_v(G)]$ are the geometric and arithmetic means respectively, of the degrees of the end-vertices of an edge. [16]The index was invented by Vukičević and Furtula was named the Geometric-arithmetic index.

Soon after the GA index was defined by using the above formula. This idea was replaced by the vertex degrees with some other vertex property. By this, the second, third, ...sixth geometric-arithmetic indices were constructed, whose chemical relevance is highly doubtful; [17] for details see reference, the reviews in references [18], [19].This index is referred to as the first geometric arithmetic index.

2.4. Randic or Connectivity Index

[20,21]Historically,the first vertex- degree - based structure descriptors were the graph invariants that nowadays are called Zagreb indices. However, initially, these were intended to be used for a completely different purpose and these were included among topological indices much later.[22] The first genuine degree-based topological index was put forward in 1975 by MilanRandic in his seminal paper,on characterization of molecular branching. His index was defined as

$$R = R(G) = \sum_{u,v \in E(G)} \frac{1}{\sqrt{d_u.d_v}}$$

Randic himself named it branching index,[23,24]but soon it was renamed as connectivity index. Nowadays, most authors refer to it as to the Randic index.

2.5. Zagreb Indices

Analysing the structure-dependency of total π-electron energyan approximate formula was obtained in which terms of the form

$$M_1(G) = \sum_{u,v \in E(G)} (d_u + d_v)$$

$$M_2(G) = \sum_{u,v \in E(G)} (d_u.d_v).$$

It was immediately recognized that these terms increase with the increasing extent of branching of the carbon-atom skeleton. i.e., these provide quantitative measures of molecular branching. Ten years later, in a review article,[25] Balaban et al. included $M_1$and M_1among topological indices and named them Zagreb group indices. The name Zagreb group index was soon abbreviated to Zagreb index, and nowadays $M_1(G)$ is referred toas the first Zagreb index, and $M_2(G)$ as the SecondZagreb index.

3. Triangulane:

[26]We intend toderive some topological indices of the triangulane$T_k$defined pictorially. We define $T_k$recursively in a manner that will be useful for our approach. First, we definerecursively an auxiliary family of triangulanes$G_k(k \geq 1)$. Let G_1 be a triangle and denoteoneofitsverticesbyy_1.We defineG_k (k≥2) asthecircuitofthegraphsGk$_{-1}$, Gk_{-1}, andK1anddenotebyykthevertexwhereK1hasbeenplaced.ThegraphsG1, G2andG3 are shown in figure 1

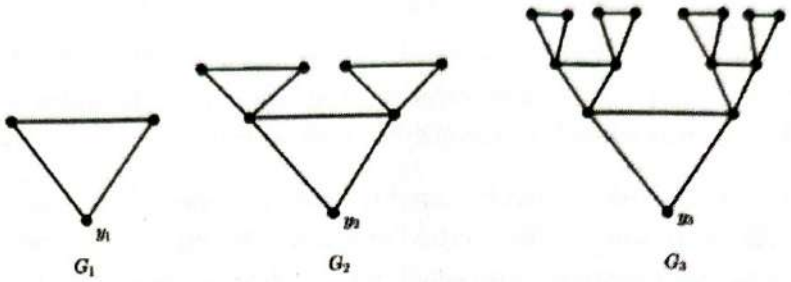

Figure1. GraphsG_1, *G2andG3*

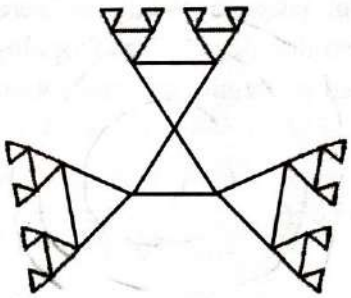

Figure2.GraphsT_3

Theorem:

For the graph$T_k(k \geq 3)$ (seeT_3 in figure 2),we have

$$H(G) = [3 + 9(2^{k-1})]\frac{1}{4} + 3(2^{k-1})\frac{1}{2} + 3(2^k)\frac{1}{3}$$

$$AZI(G) = 8[[3 + 9(2^{k-1} - 1)] + 3(2^{k-1}) + 3(2^k)]$$

$$GA(G) = [3 + 9(2^{k-1} - 1)] + 3(2^{k-1}) + 3(2^k)\frac{2\sqrt{2}}{3}$$

$$R(G) = [3 + 9(2^{k-1} - 1)]\frac{1}{4} + 3(2^{k-1})\frac{1}{2} + 3(2^k)\frac{1}{2\sqrt{2}}$$

$$M_1(G) = 72(2^{k-1} - 1) + 12(2^{k-1}) + 18(2^k) + 24$$

$$M_2(G) = 144(2^{k-1} - 1) + 12(2^{k-1}) + 24(2^k) + 48$$

Proof: Since creating such a graph is recursive, then there are$[3 + 9(2^{k-1} - 1)]$

edges withendpoints of degree 4. Also,there are $3(2^k)$edgeswithendpoints of degree 4 and 2, and there are $3(2^{k-1})$edges with endpoints of 2.

The edge set E(G) can be divided into three disjoint partitions.

$E_1 = \{e = uv \in E(G)/d_u = 4\&d_v = 4\}, |E_1| = [3 + 9(2^{k-1} - 1)]$

$E_2 = \{e = uv \in E(G)/d_u = 2\&d_v = 2\}, |E_2| = 3(2^{k-1})$

$E_3 = \{e = uv \in E(G)/d_u = 4\ \&d_v = 2\}, |E_3| = 3(2^k)$

Harmonic Index

$$H(G) = \sum_{u,v \in E(G)} \frac{2}{d_u(G) + d_v(G)}$$

$$= \sum_{u,v\ E_1(G)} \frac{2}{d_u(G) + d_v(G)} + \sum_{u,v\ E_2(G)} \frac{2}{d_u(G) + d_v(G)} + \sum_{u,v\ E_3(G)} \frac{2}{d_u(G) + d_v(G)}$$

$$= |E_1| \frac{2}{d_u(G)+d_v(G)} + |E_2| \frac{2}{d_u(G)+d_v(G)} + |E_3| \frac{2}{d_u(G)+d_v(G)}$$

$$= [3 + 9(2^{k-1} - 1)] \frac{2}{4+4} + 3(2^{k-1}) \frac{2}{2+2} + 3(2^k) \frac{2}{4+2}$$

$$= [3 + 9(2^{k-1} - 1)] \frac{1}{4} + 3(2^{k-1}) \frac{1}{2} + 3(2^k) \frac{1}{3}$$

Augmented Zagreb Index

$$AZI(G) = \sum_{u,v \in E(G)} \left(\frac{d_u(G).d_v(G)}{d_u(G) + d_v(G) - 2} \right)^3$$

$$AZI(G) = \sum_{u,v \in E_1(G)} \left(\frac{d_u(G).d_v(G)}{d_u(G) + d_v(G) - 2} \right)^3 + \sum_{u,v \in E_2(G)} \left(\frac{d_u(G).d_v(G)}{d_u(G) + d_v(G) - 2} \right)^3 + \sum_{u,v \in E_3(G)} \left(\frac{d_u(G).d_v(G)}{d_u(G) + d_v(G) - 2} \right)^3$$

$$= |E_1| \left(\frac{d_u(G).d_v(G)}{d_u(G) + d_v(G) - 2} \right)^3 + |E_2| \left(\frac{d_u(G).d_v(G)}{d_u(G) + d_v(G) - 2} \right)^3 + |E_3| \left(\frac{d_u(G).d_v(G)}{d_u(G) + d_v(G) - 2} \right)^3$$

$$=[3+9(2^{k-1}-1)]\left(\frac{4\times4}{4+4-2}\right)^3+3(2^{k-1})\left(\frac{2\times2}{2+2-2}\right)^3+3(2^k)\left(\frac{4\times2}{4+2-2}\right)^3$$

$$=[3+9(2^{k-1}-1)]\left(\frac{16}{6}\right)^3+3(2^{k-1})\left(\frac{4}{2}\right)^3+3(2^k)\left(\frac{8}{4}\right)^3$$

$$=[3+9(2^{k-1}-1)](2.67)^3+3(2^{k-1})(2)^3+3(2^k)(2)^3$$

$$=[3+9(2^{k-1}-1)]8+3(2^{k-1})\,8+3(2^k)8$$

$$=8[[3+9(2^{k-1}-1)]+3(2^{k-1})+3(2^k)]$$

Geometric-arithmetic Index

$$GA(G)=\sum_{u,v\in E(G)}\frac{\sqrt{d_u(G).d_v(G)}}{\frac{1}{2}[d_u(G)+d_v(G)]}$$

$$=\sum_{u,v\in E_1(G)}\frac{\sqrt{d_u(G).d_v(G)}}{\frac{1}{2}[d_u(G)+d_v(G)]}+\sum_{u,v\in E_2(G)}\frac{\sqrt{d_u(G).d_v(G)}}{\frac{1}{2}[d_u(G)+d_v(G)]}+\sum_{u,v\in E_3(G)}\frac{\sqrt{d_u(G).d_v(G)}}{\frac{1}{2}[d_u(G)+d_v(G)]}$$

$$=|E_1|\frac{\sqrt{d_u(G).d_v(G)}}{\frac{1}{2}[d_u(G)+d_v(G)]}+|E_2|\frac{\sqrt{d_u(G).d_v(G)}}{\frac{1}{2}[d_u(G)+d_v(G)]}+|E_3|\frac{\sqrt{d_u(G).d_v(G)}}{\frac{1}{2}[d_u(G)+d_v(G)]}$$

$$=[3+9(2^{k-1}-1)]\frac{\sqrt{4\times4}}{\frac{1}{2}[4+4]}+3(2^{k-1})\frac{\sqrt{2\times2}}{\frac{1}{2}[2+2]}+3(2^k)\frac{\sqrt{4\times2}}{\frac{1}{2}[4+2]}$$

$$=[3+9(2^{k-1}-1)][\tfrac{4}{4}]+3(2^{k-1})[\tfrac{2}{2}]+3(2^k)\frac{2\sqrt{2}}{3}$$

$$=[3+9(2^{k-1}-1)]+3(2^{k-1})+3(2^k)\frac{2\sqrt{2}}{3}$$

Randic connectivity index

$$R=R(G)=\sum_{u,v\in E(G)}\frac{1}{\sqrt{d_u.d_v}}$$

$$R=R(G)=\sum_{u,v\in E_1(G)}\frac{1}{\sqrt{d_u.d_v}}+\sum_{u,v\in E_2(G)}\frac{1}{\sqrt{d_u.d_v}}+\sum_{u,v\in E_3(G)}\frac{1}{\sqrt{d_u.d_v}}$$

$$=|E_1|\frac{1}{\sqrt{d_u.d_v}}+|E_2|\frac{1}{\sqrt{d_u.d_v}}+|E_3|\frac{1}{\sqrt{d_u.d_v}}$$

$$= [3 + 9(2^{k-1} - 1)]\frac{1}{\sqrt{4\times4}} + 3(2^{k-1})\frac{1}{\sqrt{2\times2}} + 3(2^k)\frac{1}{\sqrt{4\times2}}$$

$$= [3 + 9(2^{k-1} - 1)]\frac{1}{\sqrt{16}} + 3(2^{k-1})\frac{1}{\sqrt{4}} + 3(2^k)\frac{1}{\sqrt{8}}$$

$$= [3 + 9(2^{k-1} - 1)]\frac{1}{4} + 3(2^{k-1})\frac{1}{2} + 3(2^k)\frac{1}{2\sqrt{2}}$$

Zagerb indices:

$$M_1(G) = \sum_{u,v \in E(G)} (d_u + d_v)$$

$$= \sum_{u,v \in E_1(G)} (d_u + d_v) + \sum_{u,v \in E_2(G)} (d_u + d_v) + \sum_{u,v \in E_3(G)} (d_u + d_v)$$

$$= |E_1|(d_u + d_v) + |E_2|(d_u + d_v) + |E_3|(d_u + d_v)$$

$$= [3 + 9(2^{k-1} - 1)](4 + 4) + 3(2^{k-1})(2 + 2) + 3(2^k)(4 + 2)$$

$$= [3 + 9(2^{k-1} - 1)]8 + 3(2^{k-1})4 + 3(2^k)6$$

$$= 72(2^{k-1} - 1) + 12(2^{k-1}) + 18(2^k) + 24$$

$$M_2(G) = \sum_{u,v \in E(G)} (d_u . d_v)$$

$$= \sum_{u,v \in E_1(G)}(4 \times 4) + \sum_{u,v \in E_2(G)}(2 \times 2) + \sum_{u,v \in E_3(G)}(4 \times 2)$$

$$= |E_1|(d_u . d_v) + |E_2|(d_u . d_v) + |E_3|(d_u . d_v)$$

$$= [3 + 9(2^{k-1} - 1)]16 + 3(2^{k-1})\,4 + 3(2^k)8$$

$$= 144(2^{k-1} - 1) + 12(2^{k-1}) + 24(2^k) + 48$$

CONCLUSION

Topological indices are used for example in the development of quantitative structure-activity relationships (QSARs) in which the biological activity or other properties of molecules are correlated with their chemical structure. In this paper, a generalized formula for Harmonic index, Augmented Zagreb Index, Geometric-arithmetic Index,Randic connectivity index,and Zagreb indices of Triangulane has been calculated without using the computer.

REFERENCES

[1]. H.Wiener, structural determination of the paraffine boiling points, J. Am.Chem.Soc.69 17-20 ,1947

[2].M. V. Diudea, I. Gutman, and J. Lorentz, Molecular Topology, Babes,-Bolyai University, Cluj-Napoca, Romania, 2001.

[3]. N. Trinajstic, ′ Chemical Graph Theory, Mathematical Chemistry Series, CRC Press, Boca Raton, Fla, USA, 2nd edition, 1992.

[4]. I. Gutman, Geometric approach to degree based topological indices, *MATCH Commun. Math. Comput. Chem.* 86, 11–16 (2021

[5]. R. Cruz, I. Gutman, J. Rada, Sombor index of chemical graphs, *Appl. Math. Comp.* **399** (2021) #126018.

[6]. N. Ghanbari, S. Alikhani, Sombor index of certain graphs, *Iranian J. Math. Chem.*, inpress.

[7]. H. Deng, Z. Tang, R. Wu, Molecular trees with extremal values of Sombor indices, *Int. J. Quantum Chem.*, inpress. DOI: 10.1002/qua.26622.

[8]. K. C. Das, A. S. Çevik, I. N. Cangul, Y. Shang, On Sombor index, *Symmetry* **13** (2021) #140.

[9]. Z. Wang, Y. Mao, Y. Li, B. Furtula, On relations between Sombor and other degree-based indices, *J. Appl. Math. Comput.*, inpress. DOI: https://doi.org/10.1007/s12190-021-01516-x.

[10]. S. Fajtlowicz, Congr. Numer. 60 (1987) 187.

[11]. O. Favaron, M. Mahéo, and J. F. Saclé, Discr. Math. 111 (1993) 197.

[12]. L. Zhong, Appl. Math. Lett. 25 (2012) 561.

[13]. L. Zhong, ArsCombin. 104 (2012) 261.

[14]. R. Wu, Z. Tang, and H. Deng, Filomat 27

[15]. B. Furtula, A. Graovac, D. Vukičević, J. Math. Chem. 48 (2010) 370

[16]. D. Vukičević and B. Furtula, J. Math. Chem. 46 (2009) 1369

[17]. G. H. Fath-Tabar, B. Furtula, and I. Gutman, J. Math. Chem. 47 (2010) 477.

[18]. B. Furtula and I. Gutman, in: Novel Molecular Structure Descriptors - Theory and Applications II, I. Gutman and B. Furtula (Eds.), Univ. Kragujevac, Kragujevac, 2010, pp. 137–172.

[19]. K. C. Das, I. Gutman, and B. Furtula, MATCH Commun. Math. Comput. Chem. 65 (2011) 595.

[20]. I. Gutman and N. Trinajstić, Chem. Phys. Lett. 17 (1972) 535.

[21]. I. Gutman, B. Ruščić, N. Trinajstić, and C. F. Wilcox, J. Chem. Phys. 62 (1975) 3399.

[22]. M. Randić, J. Am. Chem. Soc. 97 (1975) 6609.

[23]. L. B. Kier, L. H. Hall, W. J. Murray, and M. Randić, J. Pharm. Sci. 64 (1975) 1971.

[24] L. B. Kier and L. H. Hall, Molecular Connectivity in Chemistry and Drug Research, Academic Press, New York, 1976.

[25] A. T. Balaban, I. Motoc, D. Bonchev, and O. Mekenyan, Topics Curr. Chem. 114 (1983) 21

[26]M. H. Khalifeh, H. Yousefi–Azari, A. R. Ashrafi, Computing Wiener and Kirchhoff indices of a triangulane, *Indian J. Chem.* 47A (2008) 1503—1507.

International Journal of Physical Education, Yoga and Health Sciences (IJPEYHS)

Journal homepage : www.ijpeyhs.com

ISSN 2349- 6312 | Vol.10, Issue -1 | February 2022 / IFSJ Impact Factor - 3.225

ANALYSIS OF MARKED GRAPH OF TWO MACHINE SYSTEM PROCESSING TWO PART TYPES USING SIGN INCIDENCE MATRIX

BALAJI P

Assistant Professor of Mathematics, Sri Chandrasekharendra Saraswathy Viswa Maha Vidyalaya, Enathur, Kanchipuram

ABSTRACT

In this paper we take a Petri net model of two machine system processing of two types which is also a marked graph and we analyse it using sign incidence matrix and form siphon trap matrix.

Keywords : Petri nets, marked graphs, Flexible manufacturing systems, Sign incidence matrix.

INTRODUCTION:

Petri nets are introduced in [1][2]. Generating basis siphons and traps of Petri nets using the sign incidence matrix is discussed in [3].The analysis of marked graph are discussed in [4] [5], we take the marked graph of 2 machine system processing two part types given in [6] and analyse them using sign incidence matrix suggested in [3] [4] [5]. This paper is organised as follows.

Section I contains basic definitions on petri nets. Section II contains algorithm given in [3] [4] [5].section III contains analysis of marked graph given in 6 using sign incidence matrix section IV contains conclusions and references.

SECTION I

1.1 BASIC DEFINITIONS:

A PN is a bipartite graph, where nodes are classified as places and transitions (graphically pictured as circles and bars, respectively), and directed arcs connect only nodes of different type. Places are endowed with integer variables called tokens. More formally, a marked PN is a 5-tuple N = (P, T, F, W, M_0), where P is a finite set of places, T is a finite set of transitions, with P∩T = ∅,F⊂(PxT)U (T x P) is the incidence or flow relation (each element of F corresponds to an arc in the PN), W : F —> N \ {0} is the arc weight function, and M_0: P —> N is the initial marking (a marking M : P —> N defines the distribution of tokens in places), where N is the set of natural numbers.

It is an ordinary PN iff W admits only unitary weights. The flow arc weight information can be given In the form of matrices, namely the input (I) and output (0), or incidence (C = O — I) matrices.)The generic element ikj[okj] of the J|p|x|T|[0|p|x|T|] matrix"represents the weight of the arc from place pk to transition tj [from transition tj to place pk] (conventionally, a 0 value is associated to nonexisting arcs). The preset •X of a set of nodes X C P U T is defined as •X = [y ∈ P ∪ T\3x ∈ Xs.t.(y,x) ∈ F}. Similarly, the postset of X is defined as X • = {y ∈ P U T\3x ∈ X s.t.(x,y) ∈ F}.

A transition tj e T is said to be enabled in a marking M if M > /(*, j), where A(*J) indicates the jth column of a generic matrix A. An enabled transition may fire, yielding the marking M* = M + C(*J).

Definition 1.2: A Marked graph is a petri net in which each place as exactly one input transition and one output transition.

Definition 1.3: For a Petrinet N with n-transitions and m-places, the sign incidence matrix A = [a_{ij}]is an n x m matrix, where its entry is given as follows.

a_{ij} = + if place j is an output place of transition i.

a_{ij} = — if it is an input place of transition i.t

a_{ij} = ± if it is both input and output places of transition i (i.e. transition i and place j form a self loop) and

a_{ij}= 0 otherwise.

Definition 1.4: The addition denoted by ⊕ is a commutative binary operation on the set of four elements B = {+,-, 0, ± } defined as follows.[3][4][5]

+ ⊕ - = ±

X ⊕ x = x, For every x ∈ B

± ⊕ x = ±, For every x ∈ B

0 ⊕ x = x, For every x ∈ B

Definition 1.5 :

A subset of places denoted as Z is both siphon and trap if Z * = * Z

SECTION II

Enumeration of siphon and trap subsets of places of marked graphs

In this section we present an algorithm for marked graphs to find all subsets of places which are both siphon and trap. We define a siphon-trap matrix for marked graphs. An relation between signincidence matrix and siphon-trap matrix for marked graphs is obtained.

Theorem : 2.1 subset of k-places Z = {p1, p2> ..... pk) in a marked graph N is both siphon and trap iff the addition of k-column vectors of the sign incidence matrix of N, A⊕ A2 ⊕.....⊕ Ak contains either zero entry or ± entry where Aj denote the column vector corresponding to place P j, j = 1,2,....k.

Proof:Let A1 ⊕ A2 ⊕ ..... © Ak = V = [vj], where Vj denote the ith row of the column vector V. The following statements are obvious from the definition of sign incidence matrix and the operation ⊕.

(a) Vi = 0 means that no place in Z is an input or output place of

transition i.

(b) Vj = + means that some place in Z is an output place of transition i.

(c) v, = - means that some place in Z is an input place of transition i. and

(d) Vj = ± means that some place in Z is an input place of transition i and some place in Z is an output place of transition i.

From the above it can be seen that every transition having an output place in Z has an input place in Z iff Vi ≠ + , for every i and every transition having an input place in Z has an output place in Z iff Vi ≠ — for every i. Thus every transition having an input place in Z and an output place in Z iff Vi ≠ + or —. That is if the vector V has only either zero entry or ± entry. Thus Z is both siphon and trap iff the vector V contains only either zero or ± entries.

Definition 2.2: A + entry is said to be neutralized by adding a—entry to get a ± entry.

ALGORITHM 2.3 [3][4][5]

Input : Sign incidence matrix A of order m x n.

Step 1:Select A_j, the first column in the sign incidence matrix A, whose corresponding ‘place is denoted as $PLACE_j$.

Set recursion level r to 1

Set $V_{jr} = A_j$

Set $PLACE_{jr} = PLACE_j$

Step 2:If V_{jr} has a ± entry at i^{th} row then $PLACE_j$ is a self loop with transition t_j. Go to step 5.

Step 3:If $V_{i\ j}$ has a+ entry in the k^{th} row find a column A, which contains a^- entry at the k^{th} row.

(a) If no such column $A_g$exists, Go to step 5.

(b) If such A, exists add it to $V_{j\ r}$ to obtain $V_{j(r+1),} = V_{j\ r} \oplus A_g$, containing a ± entry at k^{th} row. Then $PLACE_{j(r+1)} = PLACE_{jr}$ U $PLACE_{\ g}$.

(c) Repeat this step for all possible nutralizing columns A_g. This gives a new set of $V_{j(r+1)}$'s and $PLACE_{j(r+!)}$'s.

Step 4:Increment r by 1. Repeat step 3 until there are no more + entries in each $V^{\wedge -}{}_{r} = A! \ 0 \ A_2 \ 0 \ .... \ 0 \ A,-_{r}$ or no neutralizing column can be found.

Step 5:Any V_{jr} without + entries and without-entries (i.e., all the entries are either zero or ±) represents both siphon and trap (By theorem). i.e., the places in $PLACEj_{\ r}$ form both siphon and trap.

Step 6:

Delete A_j

j=j+1

Output:All sets which are both siphon and trap.

SECTION III

FLEXIBLE MANUFACTURING SYSTEM.

A Flexible manufacturing system (FMS) is an integrated computer controlled configuration of machine tools and automated material handling devices that simultaneously process medium sized volumes of a variety of part types. High productivity is achieved in such system by effectively incorpariting principle of Group technology, total quality control, etc,. and following production control strategies such as manufacturing resources planning (MRP II) and just in time (JIT) production. Flexible manufacturing system is a discrete event dynamical system in which the work pieces Of various job classes enter the system asynchronously and are Concurrently, sharing the limited resources, viz., workstations, robots, MHS, buffrs and so on. Modeling ,analysis and performance evaluations studies of fame are of immense practical interest to estabilish feasibility , evaluate qualitative and quantitative performance and compare alternative fess configuration.

Consider a set of two machine m1 and m2 processing two part types j1 and j2 each part type goes through one stage o f operation and this operation can be performed or either m1 or m2 figure 1 depicts the Petri net model of the situation the places, transition have the following interpretation .

P1 : available fresh jobs.

P2 : available machine .

P3 : processi of in progress

T1 : transition indicating start of processing.

T2 : transition indicating finishing of processing .

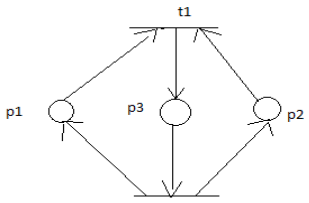

FIG 1

For the above marked graph the sign incidence matrix is given by

$$A=\frac{t_1}{t_2}\begin{bmatrix} P_1 & P_2 & P_3 \\ - & - & - \\ + & + & - \end{bmatrix}$$

Take the first column of A.By applying the above algorithm we get

$A_1 = V_{11} = \begin{bmatrix} - \\ + \end{bmatrix}$

$V_{11}^{(1)} = \begin{bmatrix} - \\ + \end{bmatrix} \oplus \begin{bmatrix} + \\ - \end{bmatrix} = \begin{bmatrix} \pm \\ \pm \end{bmatrix}$ PLACE $_{11}^{(1)} = \{P_1, P_3\}$

$A_2 = V_{21} = \begin{bmatrix} - \\ + \end{bmatrix}$

$V_{21}^{(1)}=\begin{bmatrix}-\\+\end{bmatrix}\oplus\begin{bmatrix}+\\-\end{bmatrix}=\begin{bmatrix}\pm\\\pm\end{bmatrix}$ PLACE $=\{P_2,P_3\}$

$A_3= V_{31}^{(1)}=\begin{bmatrix}-\\+\end{bmatrix}$

$V_{31}^{(2)}=\begin{bmatrix}+\\-\end{bmatrix}\oplus\begin{bmatrix}-\\+\end{bmatrix}=\begin{bmatrix}\pm\\\pm\end{bmatrix}$

$V_{31}^{(3)}=\begin{bmatrix}+\\-\end{bmatrix}\oplus\begin{bmatrix}-\\+\end{bmatrix}=\begin{bmatrix}\pm\\\pm\end{bmatrix}$ PLACE $=\{P_3,P_2\}$

The set of places which are both siphon and traphs are given by $Z_1=[p_1,p_3]$

$Z_2=[P_2,P_3]$.

DEFINITION 3.1: Let ST = $\{Z_1,Z_2,\ldots..Z_m\}$ be a set of subsets of places which are both siphon and trap of a marked graph N. Then siphon- traph matrix of N denoted as ST(N)=(a_{ij}) is a matrix where n= $|P|$, the number of places of N

a_{ij} = 1 if place j belongs to Z_i

= 0 otherwise

The siphon trap matrix of the given marked graph N is given by

$$ST(N)=\frac{Z_1}{Z_2}\begin{bmatrix}P_1 & P_2 & P_3\\ 1 & 0 & 1\\ 0 & 1 & 1\end{bmatrix}$$

Definition 3.2 : A Commutative binary operation $\circledast$ between the sets C= {0,1} and B = {0,+,-,±} is defined as

$0 \circledast X = 0 \quad x \in B$

$1 \circledast \pm = 0$

$1 \circledast X = x$ for all $x \in B - \{\pm\}$.

Definition 3.3: A commutative binary operation Θ on the set U = { 0, + , - } is defined as

0	Θ	x	=	x
+	Θ	+	=	+
-	Θ	-	=	-
+	Θ	-	=	0

THEOREM 3.4: Let ST(N) and A denote the siphon traph matrix and sign incidence matrix for a marked graph N. then $A \circledast ST(N)^T=ST(N) \circledast A^T=0$ (under Θ)

The theorem can easily verified for the above 2 matrices.

THEOREM 3.5: Let N be a marked graph with initial marking M_0. Let Z $=\{P_0,P_1,\ldots P_S\}$ be asset of places which is both siphon and trap . Then for any marking M ∈R(M_0),

$$\sum_{i=0}^{S} M(p_i) = \sum_{i=0}^{S} M_0(p_i)$$

The petri Nets fig 1 may have three types of initial markings they are M_0 = (1, 1,1) in this marking both t_1 and t_2 will be enabled and there will be a conflict therefore we can assume M^10=(0,0,1) or M_0=(1,0,1).In the first case t2 is enabled and can fire. In the Second case

t_1 is enabled and can fire.This Petri Net is live.But the token count is not the same.Therefore the above theorem is not satisfied.

We convert the above Petri Net in Fig 1 in to a directed graph by the following way.The transitions are changed in to vertices and places as edges.The arc is drawn as per the input and output relationship of the transitions.

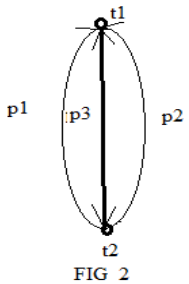

FIG 2

The above diagraph is not an Euler digraph as in degree is not equal to out degree in both the vertices. Therefore further analysis is not possible according to

SECTION IV

CONCLUSION

In this paper we took a marked graph of a two machine system processing two part types. We analyse it using sign incidence matrix and find the set of places which are both siphon and

trap. We form the siphon-trap matrix and we analyse it.we form the equivalent digraph and analyse it.

References:

1. J L Peterson, Petri nets, Department of Computer Sciences, The University of Texas, Austin, Texas 78712
2. Murata T:Petrinets: Properties, Analysis and Applications, Proceedings of IEEE,Vol.77, No.4,pp.541-580(1989)
3. Ervin R.Boer and Tadao Murata, Generating Basis Siphons and Traps of Petri Nets using the Sign Incidence Matrix, IEEE Transaction on Circuits and System-I. Fundamental Theory and Application, Vol.41, No.4,April 1994
4. K.Thirusangu and K.Rangarajan, Marked Graphs and Euler Graphs, Microelectron.Reliab. Vol.37, No.2.pp. 225-235,1997
5. K.Thirusangu and K.Rangarajan, Marked Graphs and Hamiltonian Graphs, Microelectron.Reliab. Vol.37, No.8.pp. 1243-1250,1997
6. N.Viswanadham,Y.Narahari,Coloured Petri Net Models for Automated Manufacturing Systems,IISC Bangalore,1987.
7. Narasing Deo,Graph Theory with applications to Engineering and Computer Science,Prentice Hall,India,2011.
8. Balaji P, Rangarajan K, (2015) "Analysis of Marked graph of Basic control systems and kanban control systems using sign incidence matrix", Journal of Chemicals and Pharmaceutical sciences, Special issue-9,no 38,pp 195-200.
9. Balaji P, Rangarajan K, (2015)"Marked Graphs of Basic Stock Control System and Kanban Control System and their Conversion into Digraphs", International Journal of Applied Engineering Research, Volume 10, No.80 pp 242-244.
10. Balaji P, Rangarajan K and Tamil mozhi M,(2015) "Marked Graph of Four Work Station Automated Manufacturing System and Sign Incidence Matrix", Applied Mechanics and Materials, Volume 813-814.pp1121-1125.
11. Balaji P, Rangarajan K, (2016),"Siphon and Trap Analysis of Buffer of a Flexible Manufacturing System with Three Machines and two Jobs using Sign Incidence Matrix and its digraphs", International Journal of Chemical Sciences, volume 14, no 4. pp3057-3063
12. Balaji P, Rangarajan K, (2017) "Marked Graphs of Independent Kanban Control System and Independent Extended Kanban Control System and their Conversion into Digraphs", Global Journal of Pure and Applied Mathematics, Volume 13, Number 1.pp 1-4.
13. Balaji P, Rangarajan K, (2016) "Marked Graph of Automated Manufacturing Cell with three Machines three Robots and two Part Types and its Conversion into Digraph", Transylvanian Review, Special Issue, Vol XXIV, No. 9, pp 1374-1379.
14. P. Balaji, D. Dinakar ,Analysis of Marked Graph of Cases of Deadlock Using Sign Incidence Matrix and Their Conversion into Digraphs, International Research Journal of Mathematical Sciences, Vol.7, Issue 1, 2018,PP 252-257, ISSN 2278 – 8697. 21.
15. P.Balaji G Balamurugan ,Analysis of Marked graph of cases of assembling plan using Sign Incidence Matrix and its conversion into digraphs,

International Research Journal of Mathematical Sciences, Vol.7, Issue 1, 2018, PP258-263, ISSN 2278 – 8697. 25.

16. P.Balaji I Davidraj, Analysis of Marked graph with equivalent critical place using Sign Incidence Matrix and its conversion into Digraphs, International Research Journal of Mathematical Sciences, Vol.7, Issue 1, 2018,PP264-270, ISSN 2278 – 8697. 26.
17. P.Balaji M Devarajulu ,Digraph of the Marked graphs of a Machine that process one job at at a time and basic Schema of Production State, International Research Journal of Mathematical Sciences, Vol.7, Issue 1, 2018, PP271-274, ISSN 2278 – 8697 . 27.
18. P.Balaji,M Dinesh, Analysis of Digraphs of Non-Deadlock free FMS and Machining station with Four Machines and Two Robots, International Research Journal of Mathematical Sciences, Vol.7, Issue 1, 2018, PP 275-278, ISSN 2278 – 8697. 28.
19. P Balaji,S Arumugam, Analysis of Marked Graph of Cases of Several Dependent Critical Places Using Sign Incidence Matrix and its Conversion into Digraphs International Research Journal of Mathematical Sciences, Vol.7, Issue 1, 2018, PP 279-285, ISSN 2278 – 8697. 28.
20. P Balaji,V ELumalai,Analysis of Manufacturing Cell with Four Digraph of Flexible Machines and Three Robots, International Research Journal of Mathematical Sciences, Vol.7, Issue 1, 2018, PP 286-291, ISSN 2278 – 8697. 28.
21. Balaji P Pavithra R Kirubavathy ,Analysis of a Ordinary Marked Graph Using Sign Incidence Matrix and its Conversion Into Digraphs. International Research Journal of Mathematical Sciences, Vol8, Issue 1, 2019, PP 20-26, ISSN 2278 – 8697. 28.
22. Balaji P, Ravikumar R,Analysis of MGs with Strongly Independent and Weakly Independent Places Using Sign Incidence Matrix and Their Conversion into Directed graphs,TEST Engineering and Management, Volume 83 PP 14440 - 14447 May – June 2020.
23. Balaji P, Ravikumar R Converting Four Work Station Automated Manufacturing System's Marked Graph into Digraphs and their Analysis MUKT SHABD Journal, Volume X, Issue V, pp 211-217MAY/2021.

Journal of Thermal Engineering
Web page info: https://jten.yildiz.edu.tr
DOI: 10.14744/jten.2022.xxxx

Research Article

Numerical investigation of heat transfer & hall effects on mhd nanofluid flow past over an oscillating plate with radiation

S. SARALA[1,*], E. GEETHA[2], M. NIRMALA[3]

[1]Department of Mathematics, AVIT, Vinayaka Missions Research Foundation,Chennai,Tamilnadu, India
[2]Department of Mathematics, Sri Chandrasekharendra Saraswathi Viswa Maha Vidyalaya, Tamilnadu, India
[3]Department of Mathematics, Kumararani Meena Muthiah College of Arts and Science, Tamilnadu, India

ARTICLE INFO

Article history
Received: 15 February 2021
Accepted: 29 May 2021

Keywords:
Nanofluid; Oscillating plate; Magnetohydrodynamic; Radiation; Hall Parametery

ABSTRACT

The effects of convective heat generation and the oscillatory motion of a plate in the presence of MHD, Alumina nanofluid flow, thermal radiation, and Hall current are considered. The plate oscillates harmonically in its axes with uniform temperature. The dimensional equations have to be changed into non-dimensional equations with a set of dimensionless parameters. The Laplace transformation technique is utilized to get an exact solution. The possessions of velocity and temperature are analyzed with several parameters like Prandtl number (Pr), Grashof number (Gr), Hall parameter (m), magnetic parameter (M), radiation (R), solid volume fraction(φ), phase angle(ω).The influence of primary and secondary velocity is discussed by the graph. It is observed that the increment of Hall parameter (m) diminishes the primary velocity, an increment of Grashof number leads to an increase in both velocities, and increasing solid volume fraction raises the temperature. The Nusselt number and skin friction coefficient values have expressed in the table. It is apparent that an increment of radiation increased the value of the Nusselt number and also an increment of phase angle value diminished the skin friction coefficient value.

Cite this article as: Sarala S, Geetha E, Nirmala M. Numerical investigation of heat transfer & hall effects on mhd nanofluid flow past over an oscillating plate with radiation. J Ther Eng 2022;8(6):1−15.

INTRODUCTION

A nanofluid contains colloidal suspensions of a nanometer-sized particle which is rapidly settling in fluid and stay suspended much longer than a microparticle. With the increasing influence of microprocessors and other electronic types of machinery, a pursuit for a more efficient heat-dissipating system has created nowadays an enigmatic career. Nanofluids are playing a major role in heat transfer. New prototypical nanofluids have to consider

***Corresponding author.**
*E-mail address: saralashun@gmail.com, geethamuthu06@gmail.com, nirmalswamy@gmail.com

This paper was recommended for publication in revised form by Regional Editor Tolga Taner

the surface area, size, structure-dependent behavior, and boundary resistance for thermal conductivity. The heat flux is increased by the conventional method. The automobile, electrical, and electronics companies have faced the challenges to reduce the heat level in the prototype of manufacturing. The thermal conductivity increases on the accumulation ofalumina nanofluids to normal fluids. The Alumina particle regulates the pH value in a wide range. It is an eco-friendly particle that is used in water purification and cosmetics production. Oscillating flows characterize a significant feature of conventional fluid dynamics. The oscillating plate is encouraged heat and mass transfer which is attained by fluid shaking around an immovable item or shaking of a solid form in any fluid. The Al_2O_3 nanofluid is acted as a coolant in double tube heat exchangers. It is extensively used in ceramics, nanocomposites, catalyst support, heat transfer fluids, water-resistant additives.

The numerical solution is the stability among the computational period and exactness of the solution. CongTam Nguyen et al. [1] have analyzed 36 nm and 47 nm particle size in a nanofluid. The heat and mass transmission of the vertical plate with MHD was analyzed by Muthucumaraswamy et al. [2]. Veeranna Sridhara et al. [3] reviewed Alumina nanofluid. He collected the experiment results of nanofluids which have substantially higher thermal conductivities than base fluid. The transport andthermal properties of the base fluid are converted by nanoparticles. Bhaskar Chandra Sarkar et al. [4] revealed that unsteady primary flow Hall current leads to a decrease in the amplitude of the shear stress. Lee et al. [5] experimentally inspected the thermal conductivity performance of dilute nanofluids by a transient hot-wire technique. On rotating a porous plate with chemically reactive fluid, impacts of hall current and radiation on MHD convective heat and mass transmission were contemplated by Dual pal et al. [6]. Mohammad Reza Mohaghegh [7] suggested a spectral algorithmfor the fast and competent computation of periodic flows. Siddarth Roy et al. [8]studied the heat transfer characteristics of silver/water nanofluid in a solar flat plate collector. Rajesh et al. [9] related to magnetic nanomaterial thermal flow in engineering branches and identified key development of thermal radiation heat flux in nanomaterial fabrication.

Mohaghegh et al. [10] have used periodic boundary conditions exclusively for oscillation bodies. Das et al. [11] compared Copper, Alumina, and Titania nanofluid flow with Hall effects and radiation in rotating angular velocity. Veera Krishna et al. [12] deliberated Hall effects in the oscillating porous plate with a graph that was drawn using MATHEMATICA software. Dastagiri Babu et al. [13] had instructed to neglect Hall Effect with a very small value of Reynolds number and absence of electric field. He noticed that the velocity value decreases with the increasing intensity of the magnetic parameter (M). Obulesu et al. [14] studied chemical reaction, buoyancy effects of thermal and mass diffusion with Hall effects. He assumed constant heat generation in volumetric. Hussain et al. [15] investigated the effects of Hall current and pointed out that neither energy was added nor deducted from the fluid in the electric field. Gauri Shankar Seth et al. [16]acknowledged fluid temperature and fluid velocity slowdown in ramped temperature plates instead of the isothermal plate. Sebiha Yıldız [17] has discussed the natural cooling process for reducing excess heat. He also investigated various directions at different angles of inclination for cooling a plate. Kataria et al. [18] are concerned about the heat and mass transfer of Casson fluid flow past over an oscillating plate. He analyzed the oscillating plate with ramp temperature and concentration. On the oscillating plate, Vijayalakshmi et al. [19] have explored the unchanging heat and mass flux with radiation, MHD, in presence of the chemical. Iqbal et al. [20] examined the combined reactions of radiation, Hall currents and analyzed different shapes of nanoparticles. Arifuzzaman et al. [21] considered high-speed MHD nanofluid flow with chemical reaction and radiation effect. He optimized numerical values of flow parameters and evaluated momentum and thermal boundary layer thickness. He noticed that the same order of Coriolis and viscous forces magnitude which is called Ekman layer formation near the plate.Siva Reddy et al. [22] compared the numerical values of skin friction and Nusselt number with previously published work and interpret the current values. Radha Madhavi et al. [23] have considered Alumina (Al_2O_3) nanoparticles with water and kerosene as the base fluid. Heat generation has been increased the heat transfer process and motion. Brinkman fluid had been chosen for the experiment by Arshad Khan et al. [24].Patel et al. [25] contemplated the effects of radiation, Hall current in an oscillating plate in a porous medium. He investigated isothermal temperature with the ramped wall temperature of the plate. He talked about MHD applications in various fields. He examined four different kinds of nanoparticles for computational.

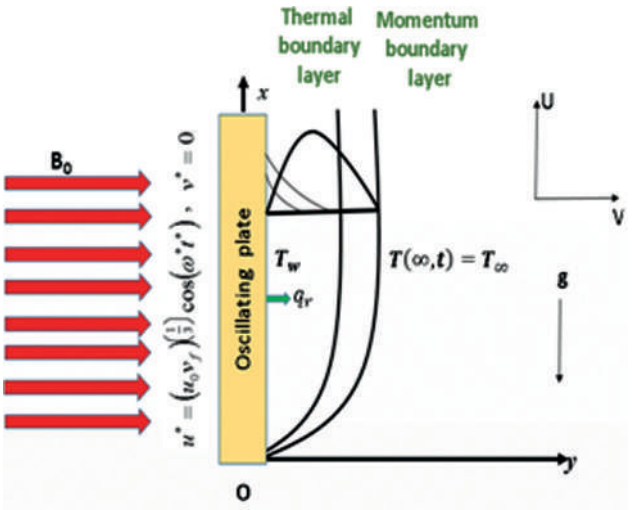

Figure 1. The physical model and coordinate system.

Dharmaiah et.al. [26] have taken Titanium alloy water-based nanofluid and a two-term analytical method applied to get a closed-form solution. Baby rani et al. [27]used Ag-water-based nanofluid and applied perturbation technique to solve nonlinear ordinary differential equations. Manjula et al. [28] carried the Dufour number with thermal radiation and chemical reaction. Balaji et al. [29] examined various cooling methods specifically the liquid cooling method with nanometer-sized particles of nanofluids. From the above literature review, they discussed the effects of particle size, the thickness of boundary layer, various nanofluid flow, different base fluid, heat reduction, MHD, radiation.

The physical model and coordinate system of a problem are shown in Figure 1.A lot of applications from the industry created important attention and motivated by the above literature review. The effects of MHD nanofluid flow of an incompressible viscous fluid past an oscillating vertical plate in the presence of Hall effects and radiation have not been studied in all the above-cited papers. In this paper, alumina-water is used.

To our knowledge, no attempts have been made to study the effects of MHD nanofluid flow of an oscillating vertical plate is considered in the presence of Hall effects and radiation.

MATHEMATICAL ANALYSIS

In the presence of thermal radiation, the viscous flow of an incompressible Al_2O_3 nanofluid past an oscillating vertical plate has been considered. The x^* oy^* the plane is taken and $z^*= 0$. At time $t \le 0$, the plate and fluid are at the same temperature T_∞. The plate has oscillated along the x^* axis and the y^* axis is normal for the remaining axes. Near the plate, the temperature value is expected T_∞. The velocity $u^* = \left(u_0 v_f\right)^{\left(\frac{1}{3}\right)} \cos\left(\omega^* t^*\right)$ is started oscillating and the temperature surges to T_W. The uniform magnetic field B_0 is applied uniformly parallel to the z^* axis. The radiative heat flux q_r is applied in the normal direction to the plate.Thermo-physical properties of water and Alumina nanoparticles are tabulated in Table 1.

The equation of continuity is $\nabla \cdot \vec{F} = 0$ where u^*, v^*, w^* denotes the components of the velocity vector $\vec{F}$. It provides $w^*= 0$ inflow which is satisfied by the plate everywhere. The external velocity varies inversely–linear with the distance along the surface which is known as Pseudo similarity. In this similarity transformation, the velocity similarity variables are taken as the core similarity variables. It is denoted by η. Thewater-based Al_2O_3 nanoparticles are taken as a fluid. The base fluid and the suspended nanoparticles are carried which are in thermal equilibrium.

Z* and t* direct the flow. The flow far away from the plate without disruption is considered.

The unstable flow of usual Boussinesq's approximation governing equations are as follows:

$$\rho_{nf}\frac{\partial u^*}{\partial t^*} = \mu_{nf}\frac{\partial^2 u^*}{\partial z^{*2}} + g(\rho\beta)_{nf}(T - T_\infty) + \frac{\sigma_{nf}B_0^2\left(mv^* - u^*\right)}{\left(1+m^2\right)} \tag{1}$$

$$\rho_{nf}\frac{\partial v^*}{\partial t^*} = \mu_{nf}\frac{\partial^2 v^*}{\partial z^{*2}} - \frac{\sigma_{nf}B_0^2\left(v^* + mu^*\right)}{\left(1+m^2\right)} \tag{2}$$

$$(\rho c_p)_{nf}\frac{\partial T}{\partial t^*} = k_{nf}\frac{\partial^2 T}{\partial z^{*2}} - \frac{\partial q_r}{\partial z^*} \tag{3}$$

where u^* is the primary velocity and v^* is the secondary velocity.

The initial and boundary conditions of the projected problem are given by:

$$\begin{aligned} &u^* = 0, \quad v^* = 0, \quad T = T_\infty \quad for\,all \quad z^*, t^* \le 0 \\ &u^* = \left(u_0 v_f\right)^{\left(\frac{1}{3}\right)} \cos\left(\omega^* t^*\right), \quad v^* = 0, \\ &\qquad\qquad T = T_w \;\; at\, z^* = 0 \;\; for\,all \;\; t^* > 0 \\ &u^* \to 0, \qquad v^* \to 0, \quad T \to T_\infty \quad at \quad z^* \to \infty \end{aligned} \tag{4}$$

On introducing the following non-dimensional quantities are:

$$U = \frac{u^*}{\left(u_0 v_f\right)^{\left(\frac{1}{3}\right)}}, \quad V = \frac{v^*}{\left(u_0 v_f\right)^{\left(\frac{1}{3}\right)}}, \quad Z = z^*\left(\frac{u_0}{v_f^2}\right)^{\left(\frac{1}{3}\right)}$$

$$\omega = \omega^*\left(\frac{v_f}{u_0^2}\right)^{\left(\frac{1}{3}\right)}$$

Table 1. Thermo-physical properties of water and Alumina nanoparticles

Physical Properties	ρ (kg / m^3)	C_p (J/KgK)	K(W / mK)	$\beta \times 10^5$ (K^{-1})	φ	σ(S/m)
Water / Base fluid	997.1	4179	0.613	21	0.0	5.5×10^{-6}
Al_2O_3 (Alumina)	3970	765	40	0.85	0.15	35×10^6

$$\theta = \frac{T - T_\infty}{T_w - T_\infty}$$

$$Gr = \frac{g\,\beta_f (T_w - T_\infty)}{u_0}$$

$$R = \frac{16\,a^*\,\sigma_f T_\infty^{\,3}}{k_f}\left(\frac{\%\rho^2}{u_0}\right)^{\left(\frac{1}{3}\right)}$$

$$\Pr = \frac{\mu c_p}{k_f}$$

$$M^2 = \frac{\sigma_f B_0^2}{\rho_f}\left(\frac{\nu_f}{u_0^{\,2}}\right)^{\left(\frac{1}{3}\right)}$$

The local radiant for the case of an optically thin gray gas is expressed by

$$\frac{\partial q_r}{\partial z^*} = -4a^*\,\sigma_f\left(T_\infty^4 - T^4\right) \tag{5}$$

It is assumed that the temperature differences within the flow are sufficiently small such that T^4 may be expressed as a linear function of the temperature. This is accomplished by expanding T^4 in a Taylor series about T_∞ and neglecting higher-order terms, thus

$$T^4 \cong 4T_\infty^3\,T - 3T_\infty^4 \tag{6}$$

By using equations, dimensionless parameter equation (3) reduces to

$$(\rho c_p)_{nf}\,\frac{\partial T}{\partial t'} = k_{nf}\,\frac{\partial^2 T}{\partial z^{*2}} + 16a^*\sigma T_\infty^3\,(T_\infty - T) \tag{7}$$

By using the dimensionless parameter, equations Eq. (1), Eq. (2), and Eq. (3) leads to,

$$L_1\frac{\partial U}{\partial t} = L_3\frac{\partial^2 U}{\partial Z^2} + L_4\frac{(U - mV)M^2}{1+m^2} + L_2 Gr.\theta \tag{8}$$

$$L_1\frac{\partial V}{\partial t} = L_3\frac{\partial^2 V}{\partial Z^2} - L_4\frac{(mU + V)M^2}{1+m^2} \tag{9}$$

$$L_5\frac{\partial \theta}{\partial t} = L_6\frac{1}{\Pr}\frac{\partial^2 \theta}{\partial Z^2} - \frac{R}{\Pr}\theta \tag{10}$$

Where

$$L_1 = (1-\phi) + \phi\left(\frac{\rho_s}{\rho_f}\right)$$

$$L_2 = (1-\phi) + \phi\left(\frac{(\rho\beta)_s}{(\rho\beta)_f}\right)$$

$$L_3 = \frac{1}{(1-\phi)^{2.5}}$$

$$L_4 = 1 + \frac{3\left(\sigma - 1\right)\phi}{\left(\sigma + 2\right) - \left(\sigma - 1\right)\phi}, \qquad \sigma = \frac{\sigma_s}{\sigma_f}$$

$$L_5 = (1-\phi) + \phi\left(\frac{(\rho c_p)_s}{(\rho c_p)_f}\right)$$

$$L_6 = \left[\frac{k_s + 2k_f - 2\phi(k_f - k_s)}{k_s + 2k_f + \phi(k_f - k_s)}\right]$$

Where R is the radiation parameter, Pr is the Prandtl number, Gr is the thermal Grashof number, and Gr approximates the ratio of the buoyancy force to the viscous force acting. Large R signifies a large radiation effect while R→0 corresponds to zero radiation effect.

The corresponding initial and boundary conditions are represented by Eq. (11),

$$\begin{gathered} U = 0, \quad V = 0, \quad \theta = 0 \quad for\,all \quad Z, t \le 0 \\ t > 0:\ U = Cos(\omega t), \quad V = 0, \quad \theta = 1 \quad at \quad Z = 0 \\ U \to 0, \qquad V \to 0, \ \theta \to 0 \ at \ Z \to \infty \end{gathered} \tag{11}$$

$$\text{Let } F = U + iV \tag{12}$$

The newest governing equations are

$$L_1\frac{\partial F}{\partial t} = L_3\frac{\partial^2 F}{\partial Z^2} - L_4\frac{F(1+im)M^2}{1+m^2} + L_2 Gr.\theta \tag{13}$$

$$L_5\frac{\partial \theta}{\partial t} = L_6\frac{1}{\Pr}\frac{\partial^2 \theta}{\partial Z^2} - \frac{R}{\Pr}\theta \tag{14}$$

The newest initial and boundary conditions are,

$$\begin{gathered} F = 0\,, \qquad \theta = 0 \ \ for\ \ all\ Z, t \le 0 \\ t > 0:\ F = Cos\left(\omega t\right), \qquad \theta = 1 \ \ at \ \ Z = 0 \\ F \to 0\,, \qquad \theta \to 0 \ \ at \ \ Z \to \infty \end{gathered} \tag{15}$$

SOLUTION PROCEDURE

The solutions are in terms of the exponential and complementary error functions. The relation connecting the

error function and its complementary error function is as follows:

$$erfc(x) = 1 - \mathrm{erf}(x) \tag{16}$$

Rajesh et al. [9] have been solved equations by the implicit finite-difference method of the Crank-Nicolson type. Vijayalakshmi et al. [19] changed partial differential equations into an ordinary differential equation using similarity transformation and applied the Runge-Kutta method to find a solution.

Laplace transformation technique is applied in the development of time-domain fluid line models, signal processing, control systems, statistical mechanics, data mining, and machine learning. Laplace transform deals with unsteady-state difficulties of transport phenomena.The standard Laplace transformation is used to solve the major dimensionless equations Eq. (13) and Eq. (14) along with conditional equations Eq. (15).The results are explained as follows

$$\begin{aligned}
F = {} & \frac{\exp(i\omega t)}{4}\begin{pmatrix} \exp(2\eta\sqrt{g(b_2+i\omega)t}) \\ erfc\left(\eta\sqrt{g}+\sqrt{(b_2+i\omega)t}\right) \\ +\exp(-2\eta\sqrt{g(b_2+i\omega)t}) \\ erfc\left(\eta\sqrt{g}-\sqrt{(b_2+i\omega)t}\right)\end{pmatrix} \\
& + \frac{\exp(-i\omega t)}{4}\begin{pmatrix} \exp(2\eta\sqrt{g(b_2-i\omega)t}) \\ erfc\left(\eta\sqrt{g}+\sqrt{(b_2-i\omega)t}\right) \\ +\exp(-2\eta\sqrt{g(b_2-i\omega)t}) \\ erfc\left(\eta\sqrt{g}-\sqrt{(b_2-i\omega)t}\right)\end{pmatrix} \\
& + \frac{c}{2d}\begin{pmatrix} \exp\left(2\eta\sqrt{gb_2t}\right)erfc\left(\eta\sqrt{g}+\sqrt{b_2t}\right) \\ +\exp\left(-2\eta\sqrt{gb_2t}\right)erfc\left(\eta\sqrt{g}-\sqrt{b_2t}\right)\end{pmatrix} \\
& - \frac{c.\exp(dt)}{2d}\begin{pmatrix} \exp\left(2\eta\sqrt{g(b_2+d)t}\right) \\ erfc\left(\eta\sqrt{g}+\sqrt{(b_2+d)t}\right) \\ +\exp\left(-2\eta\sqrt{g(b_2+d)t}\right) \\ erfc\left(\eta\sqrt{g}-\sqrt{(b_2+d)t}\right)\end{pmatrix} \\
& - \frac{c}{2d}\begin{pmatrix} \exp\left(2\eta\sqrt{abt}\right)erfc\left(\eta\sqrt{a}+\sqrt{bt}\right)+ \\ \exp\left(-2\eta\sqrt{abt}\right)erfc\left(\eta\sqrt{a}-\sqrt{bt}\right)\end{pmatrix} \\
& + \frac{c\exp(dt)}{2d}\begin{pmatrix} \exp(2\eta\sqrt{a(b+d)t})\,erfc \\ \left(\eta\sqrt{a}+\sqrt{(b+d)t}\right) \\ +\exp(-2\eta\sqrt{a(b+d)t}) \\ erfc\left(\eta\sqrt{a}-\sqrt{(b+d)t}\right)\end{pmatrix}
\end{aligned} \tag{17}$$

$$\theta = \frac{1}{2}\begin{pmatrix} \exp(2\eta\sqrt{abt})\,erfc\left(\eta\sqrt{a}+\sqrt{bt}\right) \\ +\exp(-2\eta\sqrt{abt})\,erfc\left(\eta\sqrt{a}-\sqrt{bt}\right)\end{pmatrix} \tag{18}$$

where $a = \frac{L_5\,\mathrm{Pr}}{L_6}$, $b = \frac{R}{L_5\,\mathrm{Pr}}$, $b_1 = \frac{(1+im)M^2}{1+m^2}$,

$b_2 = \frac{L_4 b_1}{L_1}$, $c = \frac{L_2 Gr}{L_1 - L_3 a}$, $d = \frac{L_3 ab - L_4 b_1}{L_1 - L_3 a}$

Dharmaiah G et.al. [26] calculated and tabulated the skin friction coefficient, Nusselt number. The dimensionless skin friction coefficient, rate of heat transfer are given as follows

$$C_f = -\left(\frac{\partial F}{\partial z}\right)_{z=0} \tag{19}$$

$$Nu = -\left(\frac{\partial \theta}{\partial Z}\right)_{Z=0} \tag{20}$$

The velocity F has computed and represented by Eq. (17). Using the below formula, the complex error function is detached from real (U) and imaginary (V) parts separately. Real and imaginary parts are differentiated with initial conditions for calculating the Nusselt and Skin friction coefficient.

$$erf(a+ib) = erf(a) + \frac{\exp(-a^2)}{2a\pi}\left[1-\cos(2ab)+i\sin(2ab)\right]$$

$$+\frac{\exp(-a^2)}{\pi}\sum_{n=1}^{\infty}\frac{\exp\left(\frac{-n^2}{4}\right)}{n^2+4a^2}\left[f_n(a,b)+ig_n(a,b)\right]+\epsilon(a,b)$$

Where $f_n = 2a - 2a\cosh(nb)\cos(2ab) + n\sinh(nb)\sin(2ab)$

$g_n = 2a\cosh(nb)\sin(2ab) + n\sinh(nb)\cos(2ab)$

$\left|\epsilon(a,b)\right| \approx 10^{-16}\left|erf(a+ib)\right|$

RESULTS AND DISCUSSION

The primary velocity (U), the secondary velocity (V) are taken in terms of parameters M, Gr, t, Pr, ω, η, m, R. The numerical calculations of respective equations are computed and represented in several graphs. The primary and secondary velocity profiles of Alumina – Water with coordinate is represented by the graph from Figure 2 to Figure 17.

Effects of Different Parameters on The Primary and Secondary Velocity Profile.

The primary velocity U decreases with an increasing value of **t** is shown in Figure 2, if ❐ =π, φ=0.15, Pr=0.71,

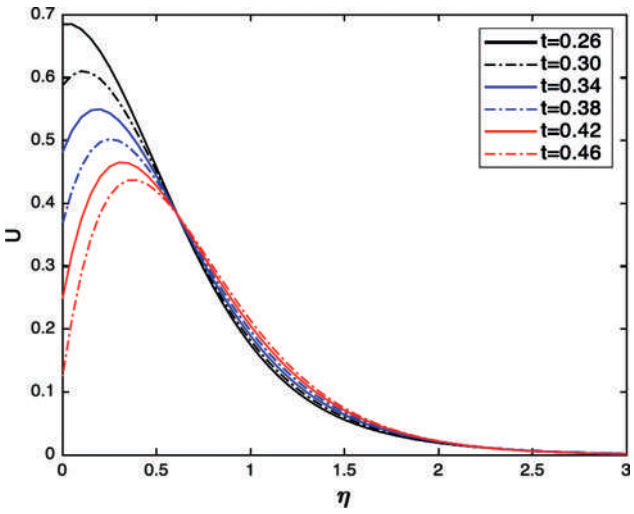

Figure 2. Primary velocity profile for various t.

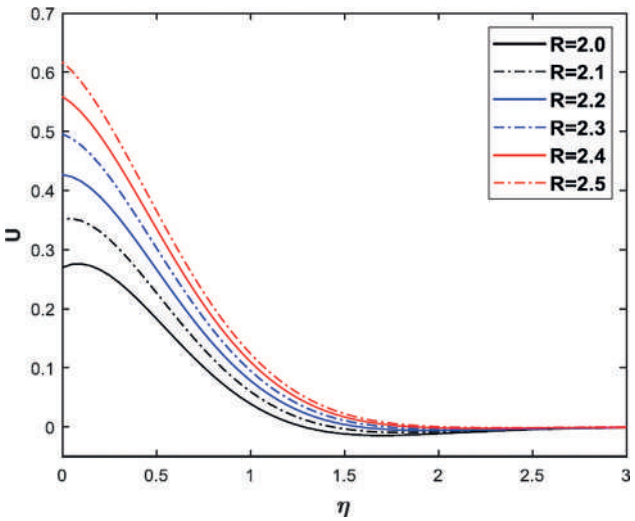

Figure 3. Primary velocity profile for various R.

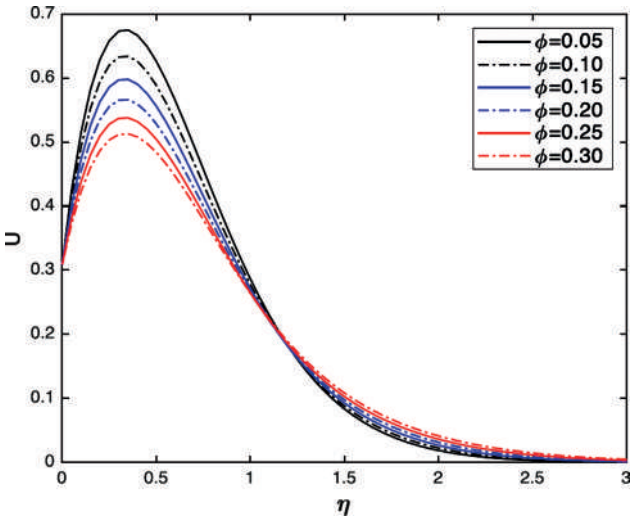

Figure 4. Primary velocity profile for various φ.

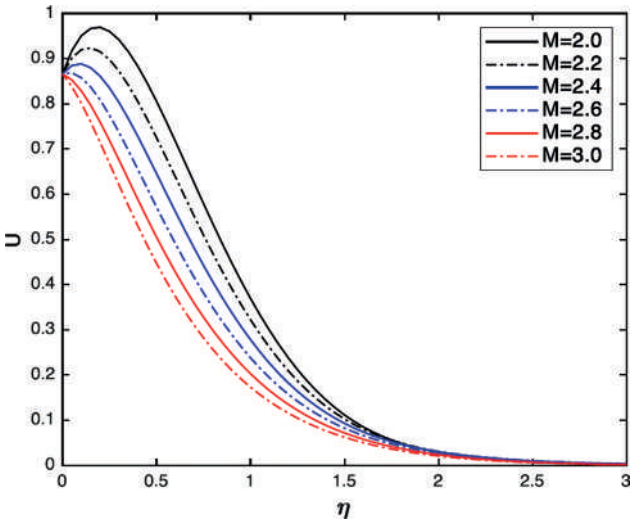

Figure 5. Primary velocity profile for a various M.

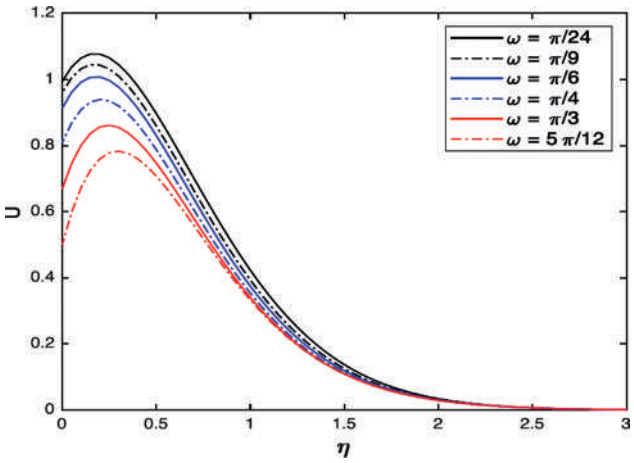

Figure 6. Primary velocity profile for various ω.

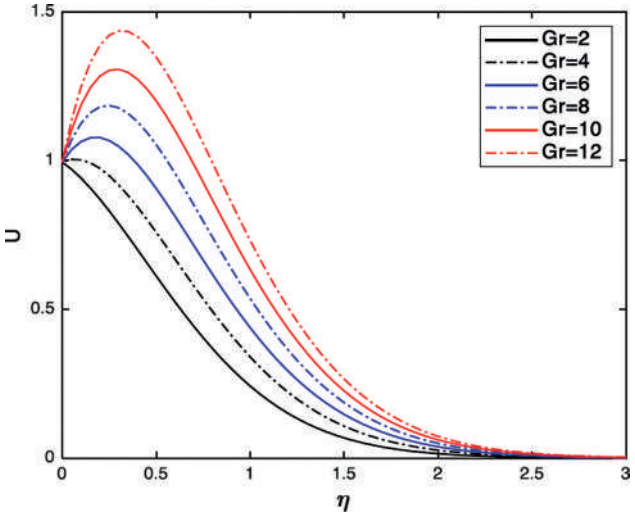

Figure 7. Primary velocity profile for various Gr.

R=0.5, t=0.26 to 0.46, Gr=3, M=1, m=1.it is observed that the secondary velocity V decreases with an increasing value of time (t) in Figure 11.

The primary velocity U and secondary velocity V increase with an increasing value of radiation (R) are illustrated in Figure 3 and Figure 16. The radiation increases the speediness of the fluid over the boundary layer field. The increment of solid volume fraction φ decreases the primary velocity U and secondary velocity V in Figure 4 and Figure 17. The density of fluid increases when nanoparticles are added to the base fluid and the fluid transforms into denser. It decreases the velocity of the fluid.

In Figure 5 and Figure 15, it is noted an increase in the magnetic field parameter (M) leads to a decrease in the primary velocity U and secondary velocity V. Due to the transverse magnetic field, Lorentz force is raised with a higher M value. It has a trend to slow down fluid motion. So both velocity is decreased with increasing values of magnetic field parameter. Baby rani et al. [27] explained Lorentz force who was resisted nanofluid flow and reduced the velocity.

In Figure 6, the phase angle ❒ increment from π/24 to 5π/12 reduced the primary velocity U. It is also noticed that the increase of phase angle has reduced the secondary velocity V in Figure 10. The velocity attains maximum

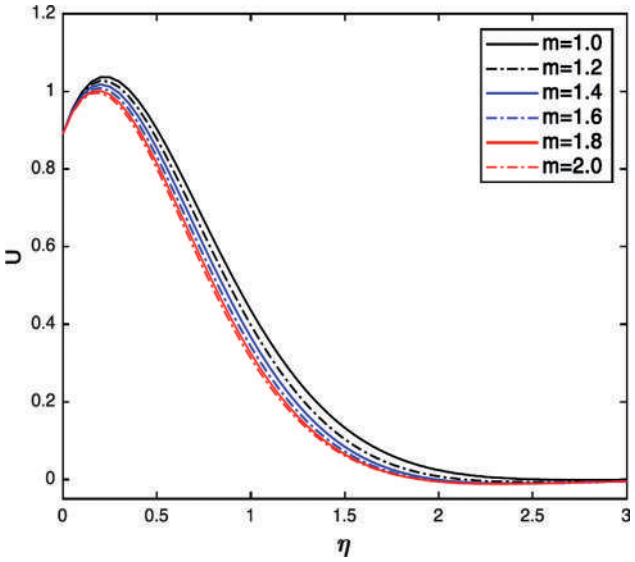

Figure 8. Primary velocity profile for various m.

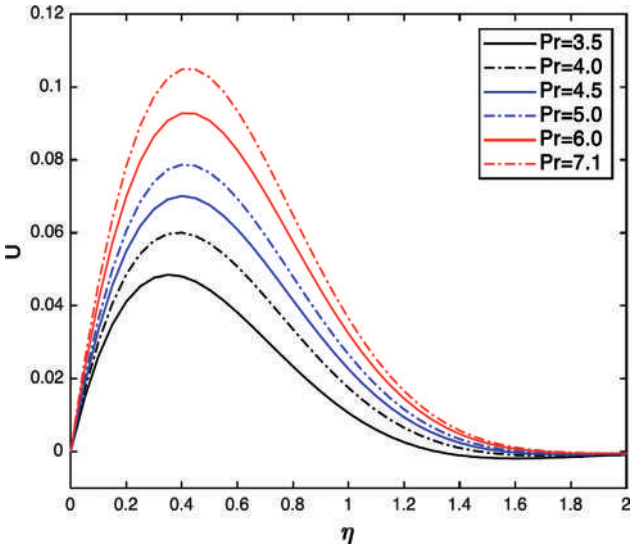

Figure 9. Primary velocity profile for various Pr.

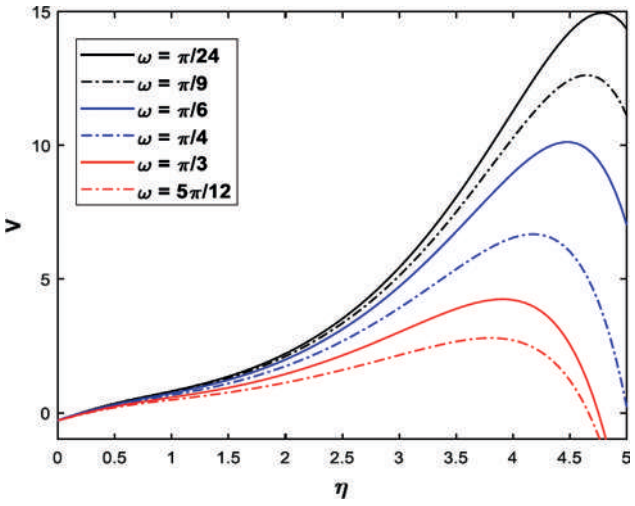

Figure 10. Secondary velocity profile for various ω.

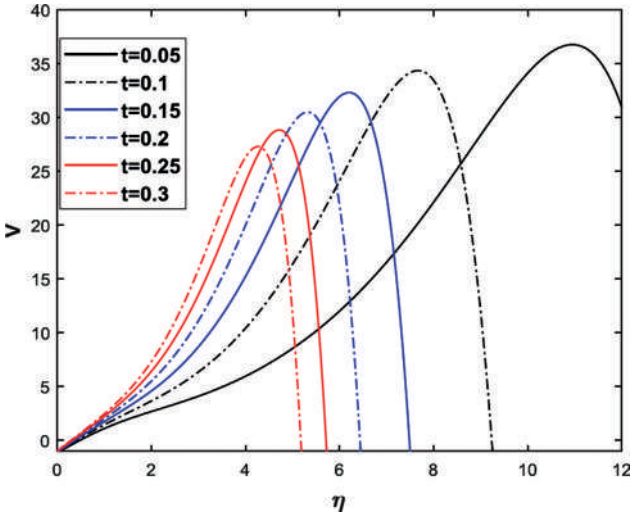

Figure 11. Secondary velocity profile for various t.

value if it is near a plate and the velocity decreasing with an increasing angle from the plate, finally approaches zero as z→ ∞.

The primary velocity U and secondary velocity V increase with an increasing value of Grashof number (Gr) are shown in Figure 7 and Figure 13. Gr is the ratio of the thermal buoyancy and viscous force that controls a fluid. The various values of Gr contribute to increasing the buoyancy force as well as decreasing the viscous forces. The fluid velocity will increase because the viscosity decreases as well as the internal resistance of the fluid decrease. In natural convection flow, the Grashof number increases the control of the flow. In the non-appearance of the free convection, the Grashof number is zero. In the cooling problem, the Grashof number has carried positive values. The cooling procedure is based on the Grashof number which is applied in the cooling of electronic components and nuclear reactors.

In Figure 8 and Figure 14, an increment of Hall parameter (m) value had reduced in Primary velocity U and secondary velocity V. Both velocity profiles decreased if m values are large, $\frac{M^2}{(1+m^2)}$ became very small then the magnetic field diminishes. An increase in *m* decreases whose active conductivity leads to magnetic restraining.

The primary velocity U and secondary velocity V increase with an increasing value of Prandtl number (Pr) are represented in Figure 9 and Figure 12. An increment

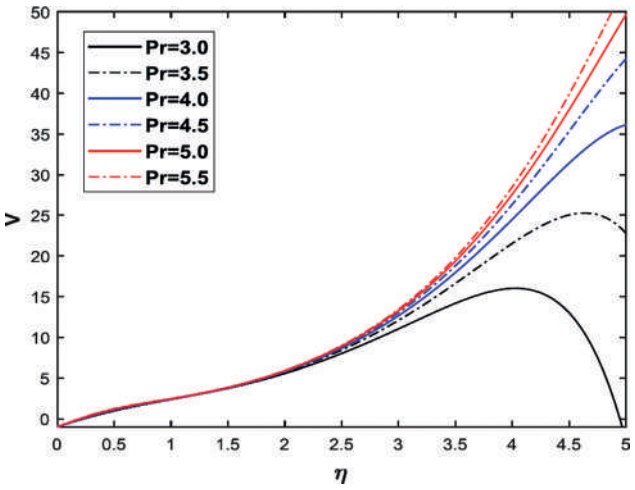

Figure 12. Secondary velocity profile for various Pr.

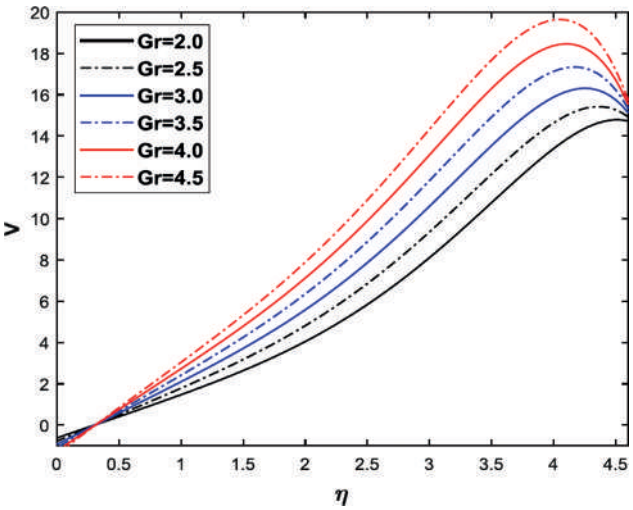

Figure 13. Secondary velocity profile for various Gr.

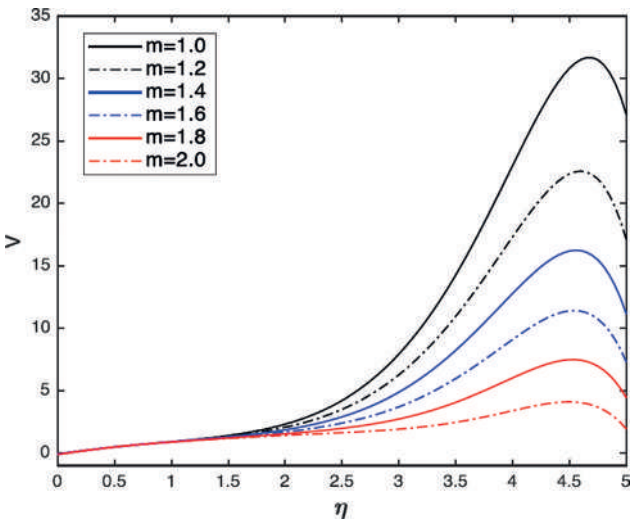

Figure 14. Secondary velocity profile for various m.

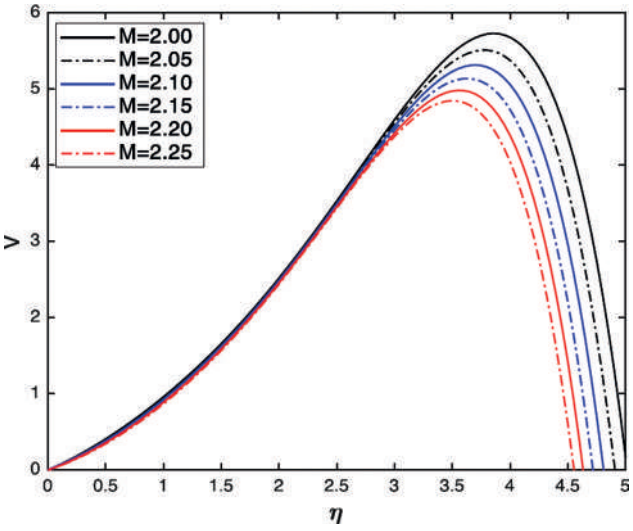

Figure 15. Secondary velocity profile for various M.

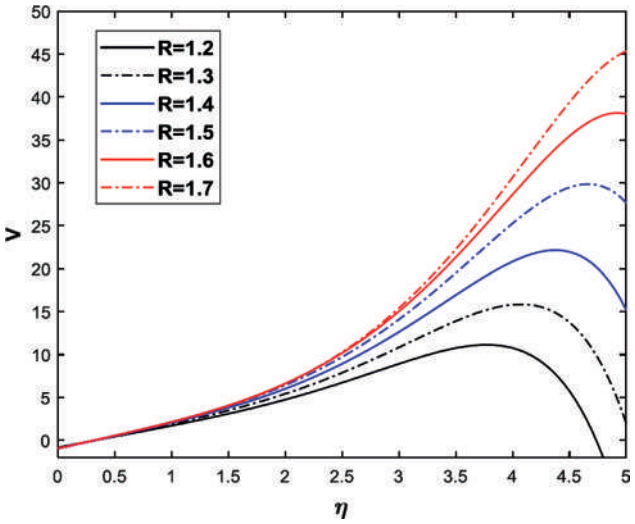

Figure 16. Secondary velocity profile for various R.

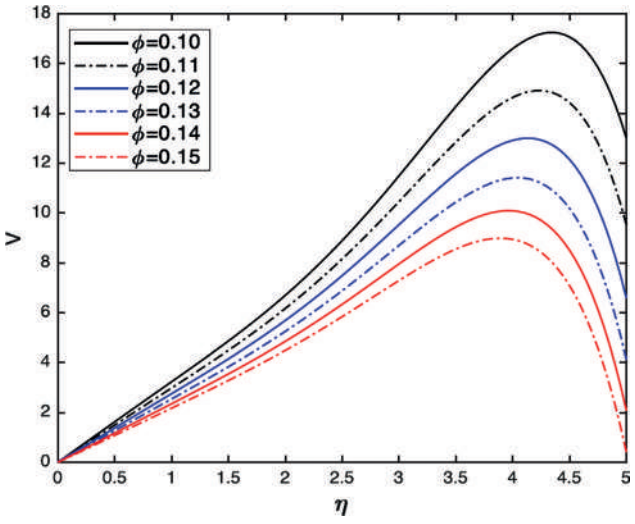

Figure 17. Secondary velocity profile for various φ

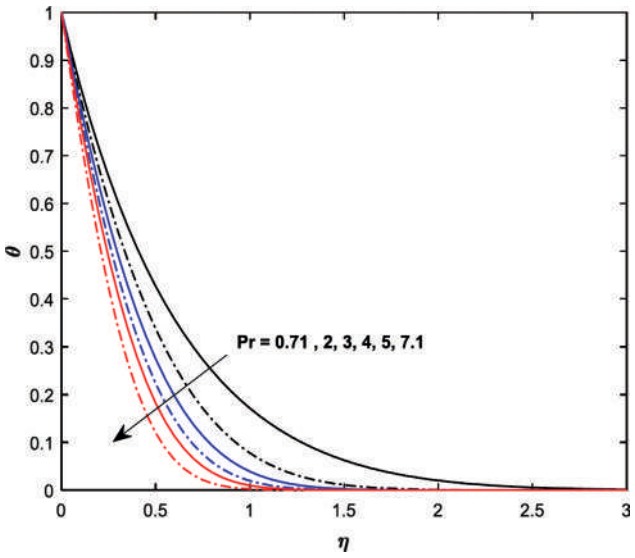

Figure 18. Temperature profile for different Pr**.**

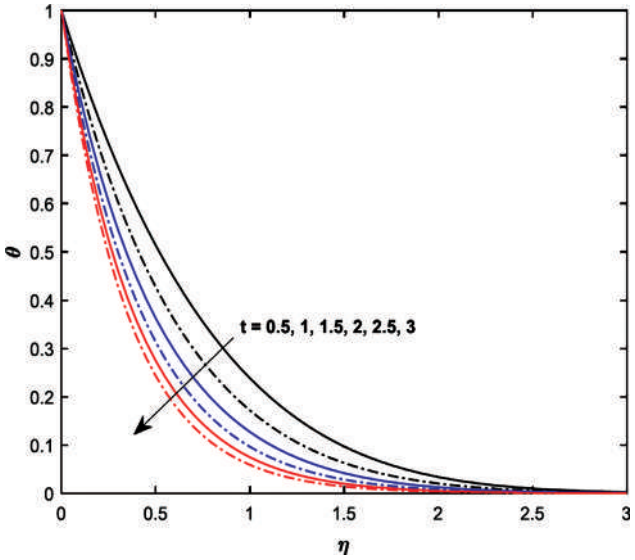

Figure 19. Temperature profile for different t.

of Prandtl number increase the Primary velocity U and secondary velocity V.Due to the Prandtl number increase, boundary layer thickness increases.it leads to an increase in the velocities.

Effects of Parameters on Temperature Profiles

The heat transfer rate is existed high in air comparing with water by Muthucumaraswamy et al. [2]. So temperature increases while decreasing the Prandtl number. The ratio of viscosity to thermal diffusivity is called the Prandtl number. An increase in thermal diffusivity points to a decrease in the Prandtl number. Thermal diffusion has a propensity to reduce the fluid temperature. The temperature profile for different values of Pr has presented in Figure 18. The temperature profile for different values of t has presented in Figure 19. It has been found that the temperature of Alumina-water nanofluid decreased with increasing values of time t.

The temperature profiles for different values of radiation parameter and solid volume fraction have shown in Figure 20. and Figure 21. It has been generated that the temperature of Alumina– Water nanofluid decreases with

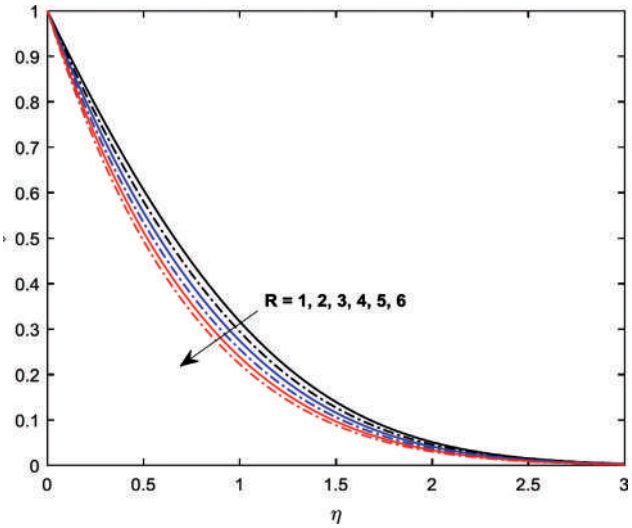

Figure 20. Temperature profile for different R.

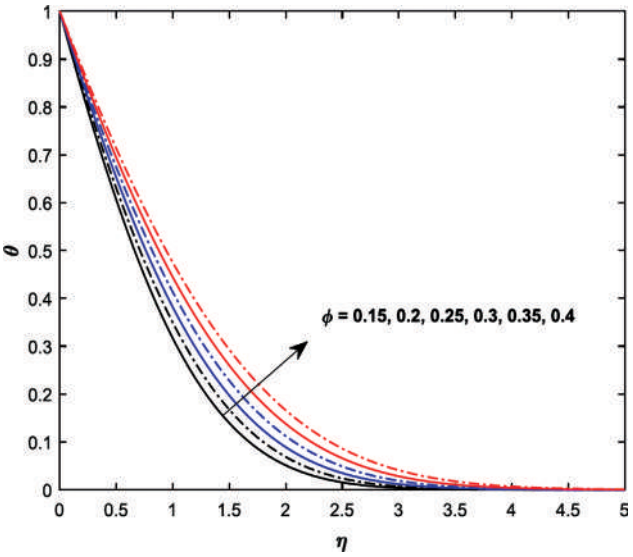

Figure 21. Temperature profile for different ☐

Table 2. Variations in Nusselt Number

t	Pr	☐	R	$-\theta'(0)$
0.5	0.71	0.15	1	1.2583
0.6	0.71	0.15	1	1.3459
0.7	0.71	0.15	1	1.4302
1.0	**0.71**	0.15	1	1.6657
1.0	**2.00**	0.15	1	1.8879
1.0	**3.00**	0.15	1	2.0754
0.1	0.71	**0.15**	1	0.8688
0.1	0.71	**0.20**	1	0.8102
0.1	0.71	**0.25**	1	0.7560
0.3	0.71	0.15	**2**	1.3459
0.3	0.71	0.15	**3**	1.5899
0.3	0.71	0.15	**4**	1.8101

Table 3. Comparison of the values of Nusselt number

☐	Ref.[5]	Present Study
0.02	1.9334	1.0492
0.04	1.7238	1.0182
0.06	1.5333	0.9885
0.08	1.3603	0.9601

increasing values of R. The temperature profile for different values of φ has displayed in Figure 21. It has been found that the temperature of Alumina-water nanofluid increases with increasing values of solid volume fraction φ.

Effects of Parameters of Skin Friction Coefficient and Nusselt Number

Friction is played a major role in a lot of engineering fields such as transportation, household usage, and measurements. Skin friction is a component of drag, the force resisting the motion of a fluid across the surface of a body. Veerakrishna et.al. [12] had calculated and listed skin friction coefficient, Nusselt number, and Sherwood number. He also revealed that skin friction increased due to an increase of urge by force and it diminished with the rise in magnetic parameter M, phase angles ω, and Grashof number. The particle size $\varphi = 0.15$ has been taken for Nusselt number and skin friction coefficient exploration.The numerical effects of solid volume fraction, radiation parameter, Prandtl number with various times on heat transfer coefficients are calculated and listed in Table.2.

From Table 2, the.Nusselt number values are gradually increased with increasing time t and t radiation R.

If Pr=0.71, Pr=2, Pr=3 then the Nusselt number values are increasing. Since free and forced convection, the Prandtl Number usage is high for heat transfer calculation with fluidproperties. In heat transfer, the Nusselt number is calculated to identify the heat transfer which is conduction or convection. The Nusselt number values of various solid volume fractions (☐) in the reference paper and the present study are shown in Table 3 which is decreasing with the increased values of particle size. In Figure 22, the Nusselt number increases with the increment of radiation

In Figure 23, Skin friction values are increased with increasing values of Hall parameter (m). The MHD flow

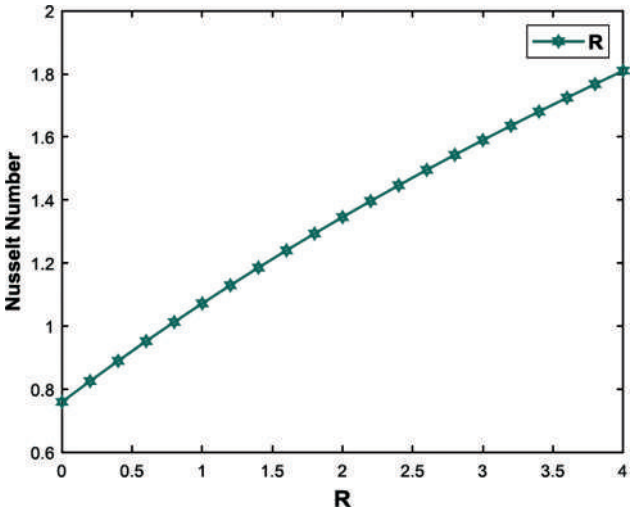

Figure 22. Nusselt number for different values of R.

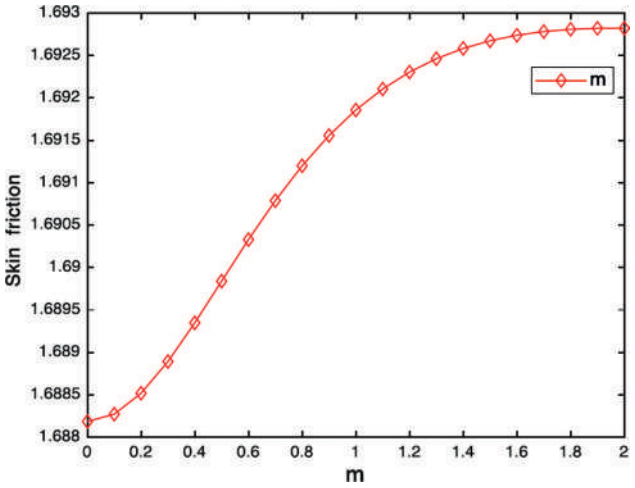

Figure 23. Skin friction coefficient for different values of m.

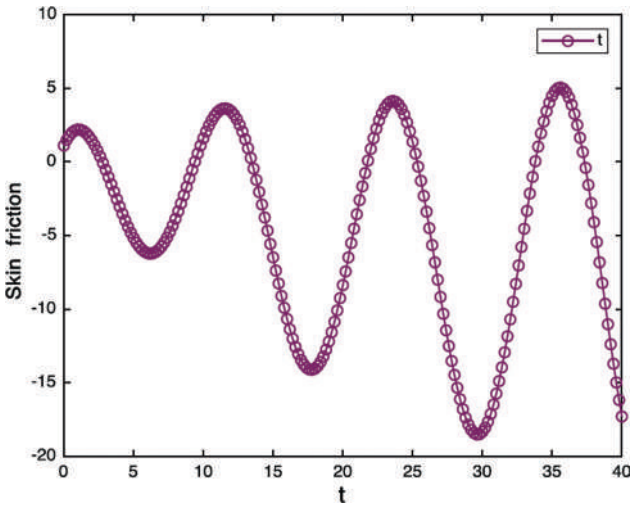

Figure 24. Skin friction coefficient values for different t in U.

with Hall current is used in the flight synchrotron. From Figure 24 and Figure 25, the Skin friction coefficient has either increased or decreased with a different time in Primary and secondary velocity. The skin friction values are compared with parameter radiation in Table 4.

The time (t), Prandtl number (Pr), Grashof number (Gr), Hall parameter (m), Magnetic parameter (M), radiation (R), phase angle (ω) parameters are considered to calculate skin friction coefficient values. It is listed in Table 5 and Table 6.

Table 4. Comparison of the values of skin friction coefficient (C_f)

R	Ref [26]	Present Study
0.02	0.8887	-0.0476
0.04	0.9032	-0.0390
0.06	0.9096	-0.0306

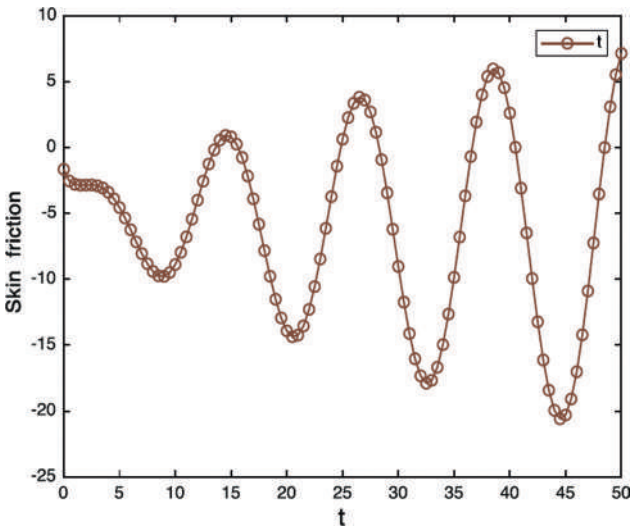

Figure 25. Skin friction coefficient values for different t in V.

CONCLUSION

The main exertion of the paper is to acquire the exact solution and to find the influence of Heat transfer and Hall Effects for the unsteady free convective Aluminananofluid flow over an oscillating plate with the existence of thermal radiation and magnetohydrodynamic. The primary and secondary velocity and temperature existence explained.

Table 5. Variations in Skin friction coefficient values of Primary Velocity (U)

t	Pr	R	m	M	Gr	❐	C_f
0.2	4.0	1.0	0.1	1.0	2.0	π/6	1.4930
0.4							1.7912
0.6							2.0058
3.6							–2.0344
3.8							–2.5403
4.0							–3.0382
0.2	**1.0**	1.0	0.6	1.0	3.0	π/3	0.8295
	1.5						0.8682
	2.0						1.5645
1	0.71	**2.0**	0.5	2	5.0	π/4	0.4745
		2.2					0.5054
		2.4					0.5344
0.2	3.0	1.2	**0.2**	0.2	4.0	π/6	1.6885
			0.3				1.6889
			0.4				1.6893
0.6	0.71	0.2	0.5	**2.0**	5.0	π/5	2.5994
				4.0			7.0455
				15.0			29.3983
0.3	2.0	0.9	0.6	1.0	**3.0**	π/7	1.6886
					11.0		2.5698
					20.0		3.5612
0.7	4.0	1.5	0.7	1.1	6.0	**π/8**	3.8620
						π/4	3.5230
						π/2	2.3037

In the probe of the oscillating plate and nanofluid flow, the highlights of concluding remarks have been summarized as followed.

- The velocity of fluid increases with the increasing values of radiation parameter, Prandtl parameter, Grashof number in both primary and secondary flows.
- The temperature of the fluid decreases with the increasing values of radiation parameter, time, and Prandtl parameter. But increasing solid volume leads to an increase the temperature.
- The Nusselt number values decrease with the increasing value of particle size.
- In primary velocity (U),the skin friction values are increased with increasing values of radiation, Hall parameter, Magnetic parameter, Prandtl number. In secondary velocity (V), the skin friction value is increased when M and ? are increased.

NOMENCLATURE

List of symbols

B_0 Constant applied magnetic field (Wbm-2)
C_p Specific heat at constant pressure (J kg^{-1} K^{-1})
C_f Coefficient of Skin Friction
E Electric field (kJ)
F Complex Function
g Gravity acceleration (ms^{-2})
Gr Thermal Grashof number
M Dimensionless magnetic field parameter
m Hall Parameter
Nu Nusselt Number
n Dimensionless frequency
Pr Prandtl number
$\bar{q_w}$ Dimensional heat flux from the plate
t^* Time(s)
t Dimensionless time (s)

Table 6. Variations in Skin friction coefficient values of secondary velocity (V).

t	Pr	R	m	M	Gr	❐	C_f
0.4	4.0	1.0	0.1	1.0	2.0	π/6	-2.2325
0.8							-2.7262
1.2							-2.8376
37.0							1.9283
37..5							4.0061
38.0							5.3854
0.2	**0.91**	1.0	0.6	1.0	3.0	π/3	-3.3957
	5.1						-7.7970
	6.5						-8.7319
1	0.71	**1**	0.5	2	5.0	π/4	0.6763
		2					0.1916
		3					-0.5366
0.2	3.0	1.5	**0.7**	2.2	4.0	π/6	-0.3228
			1.4				-0.4603
			2,1				-0.6365
0.6	0.71	0.2	0.5	**2.0**	5.0	π/5	0.4066
				17.0			5.4559
				23.0			7.3299
0.3	2.0	0.9	0.6	1.0	**9.00**	π/7	-15.1724
					27.0		-45.9262
					36.0		-61.3031
0.7	4.0	1.5	0.7	1.1	6.0	**π/8**	-12.4594
						π/4	-12.1251
						π/2	-11.5056

T Local temperature of the nanofluid (K)
T_w Wall temperature (K)
T_∞ The temperature of the ambient nanofluid (K)
$u^\star, v^\star, w^\star$ Velocity components along $x^\star$, $y^\star$, $z^\star$ axes
U, V, W Dimensionless velocity components
x, y, z Cartesian coordinates

Greek symbols
α Thermal diffusivity ($m^2 s^{-1}$)
β Thermal expansion coefficient (K^{-1})
ε Dimensionless small quantity (<<1)
φ Solid volume fraction of the nanoparticles
ρ Density
k Thermal conductivity ($m^2 s^{-1}$)
μ Dynamic viscosity (Pa s)
ϑ Kinematic viscosity ($m^2 s^{-1}$)
θ Dimensionless temperature
η Pseudo-similarity variable
ω Phase angle
σ Electrical conductivity ($m^2 s^{-1}$)

Superscript
– Dimensional quantities

Subscripts
f Fluid
nf Nanofluid
s Solid

AUTHORSHIP CONTRIBUTIONS

Authors equally contributed to this work.

DATA AVAILABILITY STATEMENT

The authors confirm that the data that supports the findings of this study are available within the article. Raw

data that support the finding of this study are available from the corresponding author, upon reasonable request.

CONFLICT OF INTEREST

The author declared no potential conflicts of interest with respect to the research, authorship, and/or publication of this article.

ETHICS

There are no ethical issues with the publication of this manuscript.

REFERENCES

[1] Nguyen CT, Roy G, Gauthier C, Galanis N. Heat transfer enhancement using Al2O3-water nanofluid for an electronic liquid cooling system. Appl Therm Eng 2007;27:1501–1506. [CrossRef]

[2] Muthucumaraswamy R, Lal T, Ranganayakulu D. Effects of rotation on MHD flow past an accelerated isothermal vertical plate with heat and mass diffusion. Theor Appl Mech 2010;37:189–202. [CrossRef]

[3] Sridhara V, Satapathy LN. Al_2O_3 -based nanofluids : A review. Sridhara Satapathy Nanoscale Res Lett 2011;6:1–16. [CrossRef]

[4] Sarkar BC, Das S, Jana RN. Effects of hall currents and radiation on MHD free convective flow past an oscillating vertical plate with oscillatory plate temperature in a porous medium. Bull Soc Math Serv Stand 2012;3:5–27. [CrossRef]

[5] Lee S, Choi S, Li S, Eastman J. Measuring thermal conductivity of fluids containing oxide nanoparticles. Heat Transf 2013;121:280–289. [CrossRef]

[6] Pal D, Talukdar B. Influence of hall current and thermal radiation on MHD convective heat and mass transfer in a rotating porous channel with chemical reaction. Int J Eng Math 2013;2013:1–13. [CrossRef]

[7] Reza Mohaghegh M. Numerical solution of linear and nonlinear periodic physical problems using fourier spectral method. J Comput Sci Comput Math 2013;3:39–48. [CrossRef]

[8] Roy S, Asirvatham LG, Kunhappan D, Cephas E, Wongwises S. Heat transfer performance of Silver/Water nanofluid in a solar flat-plate collector. J Therm Eng 2015;1:104–112. [CrossRef]

[9] Rajesh V, Mallesh MP, Sridevi C. Transient MHD nanofluid flow and heat transfer due to a moving vertical plate with thermal radiation and temperature oscillation effects. Procedia Eng 2015;127:901–908. [CrossRef]

[10] Mohaghegh MR, Rahimi AB. Three-dimensional stagnation-point flow and heat transfer of a dusty fluid toward a stretching Sheet. J Heat Transfer 2016;138:1–12. [CrossRef]

[11] Das S, Jana RN, Makinde OD. The magnetohydrodynamic free convective flow of nanofluids past an oscillating porous flat plate in a rotating system with thermal radiation and hall effects. J Mech 2016;32:197–210. [CrossRef]

[12] Krishna MV, Reddy MG. MHD Convective rotating flow past an oscillating porous plate with chemical reaction and Hall effects. IOP Conf Ser Mater Sci Eng 2016;149:012217. [CrossRef]

[13] Babu DD, Venkateswarlu S, Reddy EK. Heat and mass transfer on unsteady MHD free convection rotating flow through a porous medium over an infinite vertical plate with hall effects. AIP Conf Proc 2017;1859:87–103. [CrossRef]

[14] Obulesu M, Sivaprasad R. Hall current effects on MHD Convective flow past a porous plate with thermal radiation, chemical reaction and heat generation /absorption. Phys J 2019;2:104–125. [CrossRef]

[15] Hussain SM, Jain J, Seth GS, Rashidi MM. Free convective heat transfer with hall effects, heat absorption, and chemical reaction over an accelerated moving plate in a rotating system. J Magn Magn Mater 2017;422:112–123. [CrossRef]

[16] Seth GS, Bhattacharyya A, Tripathi R. Effect of hall current on MHD natural convection heat and mass transfer flow of rotating fluid past a vertical plate with ramped wall temperature. Front Heat Mass Transf 2017;9:1–12. [CrossRef]

[17] Yildiz S. Investigation of natural convection heat transfer at constant heat flux along with a vertical and inclined plate. J Therm Eng 2018;4:2432–2444. [CrossRef]

[18] Kataria HR, Patel HR. Heat and mass transfer in magnetohydrodynamic (MHD) Casson fluid flow past over an oscillating vertical plate embedded in a porous medium with ramped wall temperature. Propuls Power Res 2018;7:257–267. [CrossRef]

[19] Vijayalakshmi K, Umadevi R, Muthucumaraswamy R. Oscillating plate in nanofluid with uniform heat and mass flux under the effect of MHD, radiation, and chemical reaction is analyzed by Runge-Kutta method. TAGA J 2018;14:793–803. [CrossRef]

[20] Iqbal Z, Akbar NS, Azhar E, Maraj EN. Performance of hybrid nanofluid (Cu-CuO/water) on MHD rotating transport in oscillating vertical channel inspired by Hall current and thermal radiation. Alexandria Eng J 2018;57:1943–1954. [CrossRef]

[21] Arifuzzaman SM, Khan MS, Mehedi MFU, Rana BMJ, Ahmmed SF. Chemically reactive and naturally convective high-speed MHD fluid flow through an oscillatory vertical porous plate with heat and radiation absorption effect. Eng Sci Technol Int J 2018;21:215–228. [CrossRef]

[22] Sheri SR, Thumma T. Numerical study of heat transfer enhancement in MHD free convection flow over vertical plate utilizing nanofluids. Ain Shams Eng J 2018;9:1169–1180. [CrossRef]

[23] Radha Madhavi M, Nalleboyina V, Nagesh P. Influence of magnetic field, heat radiation and external surface temperature on nanofluids with different base fluids in mixed convective flows over a vertical circular cylinder. Int J Innov Technol Explor Eng 2019;8:497–504.

[24] Khan A, Khan D, Khan I, Ali F, Ul Karim F, Nisar KS. MHD flow of Brinkman type H2O-Cu, Ag, TiO2, and Al2O3 nanofluids with chemical reaction and heat generation effects in a porous medium. J Magn 2019;24:262–270. [CrossRef]

[25] Patel HR. Effects of heat generation, thermal radiation, and hall current on MHD Casson fluid flow past an oscillating plate in a porous medium. Multiph Sci Technol 2019;31:87–107. [CrossRef]

[26] Dharmaiah G, Sridhar W, Balamurugan KS, Chandra Kala K. Hall and ion slip impact on magneto-titanium alloy nanoliquid with diffusion thermo and radiation absorption. Int J Ambient Energy 2022;43:3507–3517. [CrossRef]

[27] Baby Rani CH, Vedavathi N, Balamurugan KS, Dharmaiah G. Hall and ion slip effects on ag-water based MHD nanofluid flow over a semi-infinite vertical plate embedded in a porous medium. Front Heat Mass Transf 2020;14:1–11. [CrossRef]

[28] Manjula V, Sekhar KVC. Effects of hall current, Dufour on unsteady MHD chemically reacting Casson fluid flow over an inclined oscillating plate with thermal radiation. Int J Sci Technol Res 2020;9:6439–6452.

[29] Balaji T, Selvam C, Mohan Lal D. A review on electronics cooling using nanofluids. IOP Conference Series: Materials Science and Engineering, International Conference on Advances in Renewable and Sustainable Energy Systems (ICARSES 2020) 3rd-5th December, Chennai, India. 2020;1130:012007. [CrossRef]

International Journal of Physical Education, Yoga and Health Sciences (IJPEYHS)

Journal homepage : www.ijpeyhs.com

ISSN 2349- 6312 | Vol.10, Issue -1 | February 2022 / IFSJ Impact Factor - 3.225

OPENWARES IN TEACHING MATHEMATICS AT TERTIARY LEVEL

V. K. RADHAKRISHNAN

Assistant Professor of Mathematics, Sri Chandrasekharendra Saraswathi Viswa Mahavidyalaya, Enathur, Kanchipuram

ABSTRACT

Teaching is a process of transmitting resources from one to the whole and teachers, in the process, are the charioteers. Teachers remained the only source of content delivery in the past. But, the arrival of the internet revolution has paved a new way in the process of delivering the content to the stakeholders. As a result of the IT revolution, the introduction of software in teaching has been considered an innovative practice. Understanding mathematical problems have been viewed as a challenging task for the students and a tough job for the teachers over several decades. Commercial software like MATLAB and MAPLE help in solving and understanding several mathematical problems. There are Openwares available in the market which acts as an alternative to those commercial wares. This paper gives a glimpse of some Openwares in detail to teach mathematics at the tertiary level.

Keywords: *Openwares, mathematics, MATLAB, teaching, tertiary level*

1. INTRODUCTION

Mathematics education in today's world is dependent on the growth of computer technologies for teaching, learning and research in mathematics. Calculating parts in arithmetic has advanc ed from the old-fashioned four-function calculators to scientific calculators to graphing calculators and presently to computers with a polynomial math framework. The utilization of computer programs to instruct them to solve the problems is still generally uncommon but the growing body of research and the interests that recommend that its extended use is immortal.

The underlying concepts and proofs of many mathematical concepts involve hard and abstract concepts that present a precipitous hindrance for many students. Mathematics software offers both an opportunity and a challenge to present new approaches that assist students and teachers to develop a better understanding of the original concepts. They can be used to change the emphasis of learning and teaching mathematical concepts away from usual techniques and routine symbolic manipulation toward higher-level cognitive skills that focus on concepts and problem-solving. Two key indicators of deep learning and conceptual understanding are the ability to transfer knowledge learned in one task to another task and the ability to move between different representations of mathematical objects. The software allows learners to discover rules, make and test conjectures and explore the relationship between different representations of functions and other mathematical objects using a blend of visual, symbolic and computational approaches.

2. Historical Perspective

Software in Mathematics began to appear in the early 1970s and has evolved into so many advancements out of research into artificial intelligence and machine learning concepts these days. The pioneering work on developing a computer-aided program was conducted by the Nobel laureate Prof. Martin Veltman, for symbolic mathematics,

especially to calculate the High Energy Physics in 1963. The first popular software systems that are introduced in the market were Reduce, Derive, and Macsyma which are still commercially available. A free version of Macsyma called Maxima is actively being maintained. The current market leaders are Maple, Mathematica, MatLab, SciLab and MuPAD. These are commonly used by mathematicians, scientists, and engineers.

The following table highlights some of the most popular free and commercial mathematical software. More pieces of information about them can be easily seen on their websites.

Software	***Year of Start***	***Utility***
MatLab*	Late 1970	General-purpose
Maple*	1985	General-purpose
MathCAD*	1985	General-purpose
GP/PARI	1985	Number Theory
GAP	1986	Group Theory, Discrete Math
Gnuplot	1986	Plotting software
MuPAD*	1993	General-purpose
Magma*	1993	Arithmetic Geometry, Number Theory
Octave	1993	Numerical computations, Matlab-like
R	1993	Statistics
SciLab	1994	General-purpose CAS
Macaulay2	1995	Commutative Algebra, Algebraic Geometry
CoCoA	1995	Polynomial Calculation
Singular	1997	Commutative Algebra, Algebraic Geometry
Mathematica*	1998	General-purpose
Maxima	1998	General-purpose
YACAS	1999	General-purpose
Dynamic Solver	2002	Differential Equation
GeoGebra	2002	Draw Geometric and Algebraic objects
SAGE	2005	Algebra and Geometry Experimentation
Kash/Kant	2005	Algebraic Number Theory

Here star (*) ones are commercial software and the remaining are free software. Note that the above list is not complete still and there may be many more mathematical software.

3. Teaching Applications of Some Openwares

In this paper, we are going to discuss the usage of some Openwares that are used to teach Mathematics for tertiary level students. Teaching mathematics with software helps the student to understand the concepts more and helps them to visualise everything that they solve in front of their eyes.

3.1 Microsoft Mathematic

With the Microsoft Mathematics Add-in for Word and OneNote, one can perform mathematical calculations and plot graphs in Word documents and OneNote notebooks. The add-in also provides an extensive collection of mathematical symbols and structures to display formatted mathematical expressions. Also, quickly it helps to insert commonly used expressions and math structures by using the Equation gallery. Some of the usability of the add-in is listed below:

- Compute standard mathematical functions, such as roots and logarithms
- Compute trigonometric functions, such as sine and cosine
- Find derivatives and integrals, limits, sums and products of series
- Perform matrix operations, such as inverses, addition, and multiplication
- Perform operations on complex numbers
- Plot 2-D graphs in Cartesian and polar coordinates
- Plot 3-D graphs in Cartesian, cylindrical, and spherical coordinates
- Solve equations and inequalities
- Calculate statistical functions, such as mode and variance, on lists of numbers
- Factor polynomials or integers

- Simplify or expand algebraic expressions

3.2 MegaStat

MegaStat for Excel is a full-featured Excel add-in that performs statistical analyses with an Excel workbook. It helps the user to solve all the statistical related problems all in one place. It performs basic functions, such as descriptive statistics, frequency distributions, and probability calculations as well as hypothesis testing, ANOVA, regression, and more. MegaStat output is carefully formatted and ease-of-use features include Auto Label Detect and Auto Expand for quick data selection.

3.3 Analysis ToolPak

For solving and developing complex statistical or engineering analyses, an add-in called, Analysis ToolPak from Microsoft Excel helps in saving steps and time. When the data is provided with parameters for each analysis, using the appropriate statistical tool or engineering macro functions to calculate and the results are displayed in an output table in a form of a separate sheet in the same Workbook immediately with one click. Some tools generate charts in addition to output tables.

The data analysis functions can be used on only one worksheet at a time. When performing data analysis on grouped worksheets, the results will appear on the first worksheet and empty formatted tables will appear on the remaining worksheets. To perform data analysis on the remainder of the worksheets, recalculate the analysis tool for each worksheet. The Analysis ToolPak includes the tools described in the following sections:

• Descriptive Statistics • Exponential Smoothing • Correlation • Regression • Covariance • ANOVA • F-test Two-Sample for Variance • Fourier Analysis	• Histogram • Moving Average • Random Number Generation • Rank and Percentile • Sampling • t-test • z-test

3.4 GeoGebra

GeoGebra is a completely free program which allows the user to draw geometric and algebraic objects (shapes and graphs) and investigate their properties quickly and easily. It can be downloaded from the website www.geogebra.org, where one can also use a web-based version of the program, or browse GeoGebra files others have created. Using GeoGebra, one can draw graphs by typing the mathematical equation directly into the input bar, generate shapes and common constructions easily, and on the same canvas if needed. The basic functions are fairly easy to pick up, so it is encouraging to play around with the program.

4. Conclusion

Software is a tool and not a self-contained learning package or encyclopaedia of mathematical knowledge. It is the way in which it is presented to and used by students that determine its ability to influence learning. Much emphasis these days is placed on student-centred learning and less on the teaching but teaching and learning are equally important. It is necessary to first understand the learning process and then design teaching and learning activities to achieve these. Only then will students become deep learners. There are many implications of using computers in the teaching and learning of mathematics at the tertiary level. In this paper, some of the Openwares for

mathematics education have been highlighted and shown the things that are being used for the purpose/result upon the necessities.

References

- Kumar, Ajit, and S. Kumaresan. "Use of mathematical software for teaching and learning mathematics", ICME 11 Proceedings (2008): 373-388.
- Cretchley P., (2002) Mathematics and technology: How integrated is this learning partnership, Proceedings of the Vienna International Symposium on Integrating Technology into Mathematics Education, Vienna.
- Majewski M., (2004), Seeing Is Believing: Reflections on the use of Computer Graphics in Teaching Mathematics (Part II), CASTME International and CASTME Europe Conference, Cyprus.
- Westermann T., (2000), Teaching Mathematics using a Computer Algebra, The International Journal of Computer Algebra in Mathematics Education.

A COMPARISON WITH GREEN'S RELATION AND OUR MORE SPECIAL RELATIONS

ABSTRACT

David Mclean[2] has managed to decomposition of a band into additional specialty ensembles. He created a band by semilattice union of rectangular bands. We have made an effort to create a Near idempotent semigroup as a union of more specific Near idempotent semigroups in response to this conclusion. For this reason, we changed the Mclean relations L and R into λ and ρ before moving on to define δ as C, which is also the same as ρ ∘ λ, as inspired by Green's 𝒟[3].

Keywords: *decomposition of a band, semilattice, rectangular band,* left/right singular near idempotent semigroup.

Introduction:

Our introduction of relations λ, ρ on a near idempotent semigroup is inspired by McLean's relations *L* and *R* defined on a band respectively. This exercise's goal is to break down a generic Near idempotent semigroup decomposition, more specialised one. Each δ-class is a near idempotent semigroup into rectangular near idempotent semigroup, and each λ(ρ) -class is a left/right singular near idempotent semigroup. Finally, we demonstrate that the relations λ, ρ, δ and ξ are nothing more than the extensions of the relations of green $\mathcal{L}, \mathcal{R}, \mathcal{D}$ *and* $\mathcal{H}$..

Preliminaries and Notations

Definition -Idempotent

If ee = e (e^2 = e), then element e of a semigroup S is referred to be an idempotent element of S.

Zero elements and one-sided identities are idempotent.

The opposite is typically untrue.

Definition

let S be a semigroup and 'a' an element of S. 'a' is said to be a **near – idempotent element** of S if xa^2y = xay for all x, y in S.

A semigroup S is called a **near idempotent semigroup** if every element of S is near idempotent element of S.

In any semigroup S, the left (right, two – sided) identity elements and the left (right, two – sided) zero elements are idempotents.

Definition - Band

If every element of a semigroup S is idempotent we shall say that S itself is idempotent , or that S is a **band**. (Klein – Barmen 1940)

T N KAVITHA,

Assistant Professor of Mathematics, Sri Chandrasekharendra Saraswathi Viswa Mahavidyalaya, Kanchipuram, TamilNadu,

tnkmaths@gmail.com

A COMPARISON WITH GREEN'S RELATION AND OUR MORE SPECIAL RELATIONS

Definition - Semi – lattice

A commutative band is called a **semi – lattice.**

Definition - rectangular band

Let a and b be any two non – empty sets. Then, the system S = (A × B, *) where (a,b) * (a', b') = (a, b')

For all a, a' in A and b, b' in B is a band. It is called a **rectangular band** or an **anti-commutative band**.

Green's relations $\mathcal{L}, \mathcal{R}, \mathcal{D}$ *and* $\mathcal{H}$.

Let S^1 for each semigroup S be a semigroup generated from S by adjoining an identity if S does not already contain an identity, and let S^1 Equal S otherwise. The equivalence relations on the set S that Green first developed are known as the "Green's relations of S."

According to such definitions, the L - relation as follows.

For any $a, b \in S$, $a\ L\ b$ if and only if $S^1a = S^1b$, or equivalently, $a\ L\ b$ if and only if $a = xb$ and $b = ya$ for some $x, y \in S^1$.

Dually, the R - relation defined as follows.

$a\ R\ b$ if and only if $aS^1 = bS^1$, or equivalently, $a\ R\ b$ if and only if $a = bx$ and $b = ay$ for some $x, y \in S^1$.

Moreover, the J - relation defined as follows.

$a\ J\ b$ if and only if $S^1\ aS^1 = S^1\ bS^1$,

or equivalently, $a\ J\ b$ if and only if $a = xby$ and $b = uav$ for some $x, y, u, v \in S^1$.

Finally, we define $H = L \cap R$ and $D = L \circ R$, where $\circ$ is the composition of relations. Since the relations L and R commute, it follows that $L \circ R = R \circ L$.

Special relations similar to Green's relations $\mathcal{L}, \mathcal{R}, \mathcal{D}$ *and* $\mathcal{H}$.

We first define the dual relations λ and ρ on a near idempotent semigroup in the following.

Definition

Let S be a near- idempotent semigroup and a and b, elements of S. We define the relations λ and ρ on S as follows:

a λ b if and only if xaby = xay and xbay = xby for all x, y ∈ S

a ρ b if and only if xaby = xby and xbay = xay for all x, y ∈ S.

Both λ and ρ turn out to be equivalence relations on S. It is easy to check that λ is a right congruence and ρ is a left congruence relation on S.

Lemma

Let S be a near idempotent semigroup. Then the relation λ is an equivalence relation on S.

Proof $xa^2y = xay$ for all x, y , a ∈ S, by the definition of near- idempotent semigroup, so that a λ a for all a in S.

Hence λ is reflexive.

Let a λ b.

A COMPARISON WITH GREEN'S RELATION AND OUR MORE SPECIAL RELATIONS

Then $xaby = xay$ and $xbay = xby$ for all $x, y \in S$

which also implies $b \lambda a$.

Hence λ is symmetric.

Let $a \lambda b$ and $b \lambda c$

Then for all $x, y \in S$,

we have, $xaby = xay$, $xbay = xby$ and $xbcy = xby$, $xcby = xcy$

Hence $xacy = x\,a\,cy = x\,ab\,cy = x\,a\,bc\,y = x\,ab\,y = xay$ for all $x, y \in S$

Similarly,

$xcay = x\,cb\,a\,y = x\,c\,ba\,y = x\,c\,b\,y = xcy$ for all $x, y \in S$,

Which implies $a \lambda c$. Hence λ is transitive.

Thus λ is an equivalence relation on S.

Dually, We can prove that ρ is an equivalence relation on the near - idempotent semigroup S.

We now prove that λ is a right congruence and ρ is a left congruence relation on S.

The following theorem shows that λ is a right congruence relation on S.

Lemma

Let S be a near – idempotent semigroup. Let $a \lambda b$. Then $ac \lambda bc$ for all $c \in S$

Proof

Let $a \lambda b$ where $a, b \in S$.

We claim that for any $c \in S$, $ac \lambda bc$.

$a \lambda b \Rightarrow xaby = xay$ and $xbay = xby$ for all $x, y \in S$

Then for all $x, y \in S$, we have

$xac\,bcy = xa\,cbc\,y = xab\,cbc\,y = x\,a\,(bc)^2\,y = xabcy$ (by the definition of S) $= xab\,c\,y = xacy$

and

$x\,bc\,ac\,y = x\,b\,cac\,y = x\,ba\,cac\,y = xb\,(ac)^2\,y = x\,b\,ac\,y$ (by the definition of S) $= x\,ba\,c\,y = x\,bc\,y$

Leading to $ac \lambda bc$ for all $c \in S$, Hence λ is a right congruence on S.

Dually, ρ is a left congruence relation on S.

We now consider the composition of the two relations λ and ρ and prove that . $\lambda \circ \rho = \rho \circ \lambda$.

Lemma:

If S is a near- idempotent semi group, then $\lambda \circ \rho = \rho \circ \lambda$ in S.

Proof :

We first prove that $\lambda \circ \rho \subset \rho \circ \lambda$.

Let $a \lambda \circ \rho\ b$.

Then there exists $c \in S$ such that $a \lambda c$ and $c \rho b$.

$a \lambda c \Rightarrow xacy = xay$ and $xcay = xcy$ for all $x, y \in S$.$c \rho b \Rightarrow xcby = xby$ and $xbcy = xcy$ for all $x, y \in S$.

Choose $d = acb$.

Then for all x, y in S,

A COMPARISON WITH GREEN'S RELATION AND OUR MORE SPECIAL RELATIONS

xady = x a acb y = x a^2 cb y = x a cb y = x acb y = xdy

xday = x acb ay = x ac bay

= x a b ay

= xab a y

= xab ac y

= xacy (since ρ is a left congruence ab ρ ac)

But xacy = xay,

so that finally we get xday = xay

Therefore a ρ d

Similarly,

xdby = xacbby = xacb^{2}y = xacby = xdy for all x, y in S.

xbdy = x b acb y = xba cb y = xba b y = x b aby = x cb aby = xcby

(since λ is a right congruence ab λ cb)

But xcby = xby,

so that we get xbdy = xby

Hence d λ b

Thus a ρ d, d λ b so that a ρ λ b

This gives $\lambda \circ \rho \subset \rho \circ \lambda$

By a similar argument,

We can prove that

$\rho \circ \lambda \subset \lambda \circ \rho$ Thus we get $\lambda \circ \rho = \rho \circ \lambda$

We now define the relation δ on S as follows

Definition:

Let S be a near- idempotent semigroup. Let a, b ∈ S. we define $\delta = \lambda \circ \rho$. In other words, a δ b if and only if there exists c ∈ S Such that a λ c and c ρ b.

We have already proved that $\lambda \circ \rho = \rho \circ \lambda$. Hence w e can write a $\lambda \circ \rho$ b or a $\rho \circ \lambda$ b instead of a δ b.

We now prove that δ is an equivalence relation on the near – idempotent semigroup S.

Lemma

Let S be a near idempotent semigroup. δ is an equivalence relation on S.

Proof:

For all a in S, a λ a and a ρ a since λ and ρ are reflexive,

so that a $\lambda \circ \rho$ a, which means a δ a.

Hence δ is reflexive.

a δ b $\Rightarrow$ a $\lambda \circ \rho$ b

There exists u ∈ S such that a λ u and u ρ b

There exists u ∈ S such that b ρ u and u λ a since λ and ρ are symmetric

$\Rightarrow$ b $\rho \circ \lambda$ a $\Rightarrow$ b δ a

(since $\lambda \circ \rho = \rho \circ \lambda = \delta$)

Hence δ is symmetric.

a δ b, b δ c

$\Rightarrow$ There exist u, v $\in$ S such that a λ u and u ρ b; b λ v and v ρ c

Since u ρ b and b λ v

we have u $\rho \circ \lambda$ v

We have u $\lambda \circ \rho$ v since $\lambda \circ \rho = \rho \circ \lambda$

Thus there exists w $\in$ S such that u λ w and w ρ v

a λ u and u λ w so that a λ w;

w ρ v and v ρ c so that w ρ c

Therefore a $\lambda \circ \rho$ c

i.e, a δ c. Thus δ is transitive. Hence δ is an equivalence relation on the near- idempotent semigroup S.

Conclusion

We demonstrate that the relations π and δ coincide on the near-idempotent semigroup S by defining the relation π on S in a manner similar to David McLean's relation P defined on a band[22]. In contrast to Green's, our relationship is more unique.

References

1. Chollawat Pookpienlert [1] , Preeyanuch Honyam [2], and Jintana Sanwong [2] , Green's Relations on a Semigroup of Transformations with Restricted Range that Preserves an Equivalence Relation and a Cross-Section, 4 August 2018 , Mathematics 2018, 6, 134; doi:10.3390/math6080134 , www.mdpi.com/journal/mathematics.*

2. David Mc Lean, D.,Idempotent Semigroups, Am. Math. Mon. 61 (1954). 110-113

3. Green J.A. , On the structure of semigroups, Ann. of Math. 54 (1951), no. 1, 163–172.

4. Howie, J.M. Fundamentals of Semigroup Theory; Oxford University Press: New York, NY, USA, 1995

5. Sanwong, J.; Sommanee, W. Regularity and Green's relations on a semigroup of transformations with restricted range. Int. J. Math. Math. Sci. 2008.

Sanwong, J.; Singha, B.; Sullivan, R.P. Maximal and minimal congruences on some semigroups. Acta Math. Sin. Engl. Ser. 2009, 25, 455–466.